To-do list:

In `{12_introduction.tex}`:

- WM drift/allan deviation
- Laser scanning infrastructure
- Setpoint errors, allan plot
- Diagnostic logging
- Possible improvements to system

In `{20_metrology.tex}`:

- Find old notebooks for polarization writeup
- Read Rengelink thesis in detail

In `{21_transitions.tex}`:

- Paper: Tidy up future directions.
- Paper: Cite proton radius puzzle papers esp Wim's group
- Ensure existing segments fairly complete and flow alright.
- What sources of lorentzian broadening exist? Or narrowing?!
- What about the other lines he measured? Were they all systematically off?
- Did he find similar transition strengths, or is this also a factor?
- Sequence diagram
- Do the damn modelling:, 2^3P population, 3level model, Evaporative cooling model, Estimate sensitivity to photon scatterings, Upper state lifetimes?
- Get data for AOM and RF calibration
- What accuracy is required for charge radii differences?

In `{31_depletion.tex}`:

- Kill redundancy
- Spend 2x half day with correlation calcs
- Make a real nice picture of a BEC...

Metrology and Many-Body Physics with Ultracold Metastable Helium

Jacob Alexander Ross

A thesis submitted to
The Australian National University
for the degree of
Doctor of Philosophy in physics

June 2016 - June 23, 2020

Metrology and Many-Body Physics with Ultracold Metastable Helium

Jacob Alexander Ross
He* BEC group
Laser Physics Centre
Research School of Physics
Joint Colleges of Science
Australian National University
Canberra, Australia

Supervisory committee: Dr Sean Hodgman
Professor Andrew Truscott
Professor Kenneth Baldwin

Declaration
Except where acknowledged in the customary manner, the material presented in this thesis is, to the best of my knowledge, original and has not been submitted in whole or part for a degree in any university.

Jacob A. Ross

Australian National University

For my parents - finally you can see me in robes.

"We who cut mere stones must always be envisioning cathedrals"
- Quarry workers' creed

Figure 1: A meme.

Contents

List of Figures

List of Tables

Part I

Preface

Précis

Prologue

This thesis documents three projects that were undertaken in the ANU Helium BEC laboratory over the period of 2018-2019 and one project, which remains unfinished, that was undertaken in 2016-2018. A number of other graduate students were in residence at the time, and each of them contributed variously to the experiments. These experiments constitute a chapter each, and conclude with acknowlegements of the contributions of each person involved. The chapters are arranged in such a way as to provide a progression through subjects of increasing complexity, and are separated into three parts.

Transitions - simplicity? Tuneout - measuring zero - the only constant is change, so can anything really have *no* effect? Depletion[**Chang2016**] - stillness, and the impossibility thereof - vacuum fluctuations Lattice - complexity Does the citation wo

The first part includes a general introduction to ultracold atomic physics and an overview of the apparatus used to complete the experiments described in this thesis.

The second part includes chapters 3 and 4, and concentrates on a pair of experiments regarding the atomic structure of Helium. The experiments in this section are motivated by open questions in atomic structure theory, and includes a review of essential concepts. Chapter 3 concerns a set of measurements of electronic absorption lines, which in some sense is the most elementary concept encountered in this thesis. Chapter 4 describes the measurement of a tune-out frequency in Helium, at which there is a null response of the atomic dipole induced by an oscillating electric field. Such tune-out frequencies are determined by the interplay of an array of atomic transitions, and so this chapter represents a marginal increase in complexity. Conversely, the signals sought in chapters 3 and 4 are presented in sequence of decreasing signal power, ultimately converging on a measurement of a null response, attempting to determine when *nothing* happens.

Following these studies of the internal structure of atoms, the third part, consisting of chapters 5 and 6, is concerned with interacting systems. Chapter 5 describes a third completed project concerning the effects of weak interactions on the density and correlations of the momentum spectrum of ultracold Bose gases. This section includes an overview of the relevant physics of ultracold gases. Chapter 6 discusses the motivation for, and progress towards, an optical lattice trap for ultracold Helium. This was the initial project of my PhD, but after two years of work the decision was made to discontinue working to construct this apparatus. Chapter 7 presents a summary of the findings of all the projects in this thesis, presents future directions of research using ultracold helium, and concludes by unraveling the narrative thread of this thesis.

Chapter 1

Introduction

1.1 Quantum degenerate gases

1.1.1 The fruits of one century

1.1.2 Theory of degenerate Bose gases

1.1.3 Distilling coherence

1.2 Metastable helium

1.2.1 Peculiarities of helium

Helium exhibits a uniquely large gap between the ground and excited states (is it the biggest? What other electronic transitions have higher energy. The lowest-lying excited state differs in electron spin from the ground state, and is also an S state, hence the transition is *doubly* forbidden. This confers a lifetime of 7900 seconds, as measured by Hodgman et al in the lab in which I started my thesis. The gap of 19.8eV is a few times the work function of most metals, which is the key enabler of the use of the delay-line detector in our experiment. However, interatomic collisions may also distribute this energy between atoms, ionizing them. What other decay channels can you have? Can both atoms remain neutral and yet disperse the 20eV in kinetic energy? This is known as Penning ionization (box: Penning and his ionization) and can lead to atom loss or sample heating. Fortunately it can be suppressed if the sample is spin-polarized, because then the scattering process no longer conserves angular momentum. The suppression, oddly, fails at very high magnetic fields - maybe because of deformation of atomic orbitals. As Penning ionization is collision-driven, the ion production scales with the square of the atomic density. This means that monitoring the ion production rate can be used as a measure for the atomic density, and indeed has been used to detect the condensation of Helium previously by this group. Also, I think people tried to use it as a feedback signal, but I dunno how that went.

The metastable gap is the agony and the ecstasy of Helium. Other noble gases also exhibit large gaps and long metastable lifetimes, but the lifetime decreases with increasing mass, and the penning ionization rate is harder to suppress. As they have larger masses, also, the condensation temperature is lower. Given the technical difficulty of condensing Helium, it may remain the only noble gas ever condensed for the foreseeable future. LEVEL DIAGRAM GOES HERE

1.2.2 Vaccum chamber

1.2.3 Diagnostics and control

1.2.4 Laser systems

The light source is a tunable M-squared Ti:Sapphire laser system. Light at 1064nm from a Lighthouse Photonics Sprout module is frequency doubled by second-harmonic

generation to pump an M-squared SolsTi:S titanium-sapphire laser which we operate around 800nm. The output from the SolsTi:S is doubled again in an M-squared ECD-X module to the target wavelengths. A fraction of the light is fed into a High Finesse WS8 wavemeter, which we calibrate with respect to the two-photon crossover transition between the $6^2P_{\frac{3}{2}}(F = 4)$ and $6^2P_{\frac{3}{2}}(F = 5)$ lines in a Cesium vapor cell. High Finesse specifies the absolute accuracy of the WS-8 at 2MHz withn 2nm of a transition line, and 10MHz otherwise. We use the wavemeter to lock the tunable laser with respect to the red light, so the uncertainty is doubled in determinations of the blue frequency. A software lock uses the wavemeter output to stabilize the laser to within 100kHz of the target wavelength. We take several scans across the target transitions by automatically updating the laser set point in the software loop.

We use the first diffracted mode of an acousto-optical modulator (AOM), driven at 189MHz, to control the beam power. The output of the AOM enters an optical fibre which couples the light to the vacuum insertion optics. The optical power is regulated with reference to a photodiode which samples the beam after the fibre via a polarizing beamsplitter. WM drift/allan deviation

The light source for our probe beam is a super-cool tunable laser which was generously loaned to us by Chris Vale's group at Swinburne uni, which is actually N lasers in series. First, a 1064nm seed is doubled by second-harmonic generation to 532nm, which is used as the pump beam for a tunable titanium-sapphire laser with a variable output that we operate within the 800nm range. This is doubled again by a nonlinear crystal to around 400nm. A fraction of the light is fed into the two ports of a High Finesse WS8 wavemeter, which we periodically calibrate with respect to a two-photon transition in a Cesium cell. This gives us a monitor for our software lock which is stable to 100kHz. We use the first diffracted order of an AOM to regulate the intensity of the light with respect to a photodiode placed after the output of the fibre that couples the laser generation table to the vacuum entry window. The profile and polarization of the beam are controlled with waveplates and lenses after a polarizing beam splitter.

- Laser scanning infrastructure
- Setpoint errors, allan plot
- Diagnostic logging
- Possible improvements to system

What is the nature of reality?

Ok so somewhere in here I wax lyrical. We tend to try to understand things. Why? Well. There is something advantageuos about being able to make predictions bout the world. This is something that has enhanced our survival prospects. But in humans something seems to be running on overdrive. And, sure, this isn't really relevant to the thesis, but you want to start from somewhere that naturally lreads to a framing of atomic theory. Matter is inescapable. Except perhaps in the dream state - we are

surrounded by substance. Some two or so thousand years ago, Democritus posited that there was a smallest thing. That one could break mountains down into boulders, boulders down to stones, stones to sand, and sand... To something indivisible. He called them, literally, atomos, for indivisible. This was astoundingly prescient: The atomic theory, as it came to be known, would not find empirical validation for another millenia or so. And, like all theories that prove to be correct, it too reached its point of failure a few hundred years thereafter. The atomic theory was outlandish at the time, breaking with the notion that things were ultimately continuous. The exploration of the atomic world eventualyl yielded a new kind of understanding of everyday matter. Kinetic theory of gases, thermodynamics, 'absolute zero'

The first profound successes were had with gases, laying the foundations for thermodynamics and the understanding of the extraction of energy from storage in chemical bonds, via heating a working fluid, say - and powering the steam revolution. Among the findings of the kinetic theory of gases was what later became known as an equation of state - an apparently universal relationship between macroscopic quantities - pressure, temperature, volume, and mass - expressing the balance of energy in gases. Among the findings that stem from this understanding was the notion of an absolute temperature scale: That if one could extract enough energy from a gas, by cooling it, then its internal energy would vanish. It would have no volume. It would be motionless. This prediction predated Einstein's formulation of the mass-energy equivalence, but even at the time, it was appreciated that gas molecules had to have a size. So they could not vanish simply by getting colder. This paradox took some years to resolve, and it was only possible by completely overturning the picture of the atom. While understanding thus far had stemmed from the investigation of matter, the first quantum revolution was to come from the study of light. Spectra & old quantum theory

Spectra are typically obtained by taking a beam of light - say, from a pinhole or slit in a mask - and passing it through a medium, such as glass, which disperses the light according to its colour. In modern parlance, there is a difference between the momentum (direction of travel) of light with different energies (related to frequency). It was by WHO? that spectra were first resolved with enough detail to distinguish more or less intense lines against an apparent continuum. And in particular, that pure elemental sources created different colours. A standard prism and screen would show different results with different elements. Wait - but by this point, we must have had an understanding of electrons, right? Because there was this Bohr model, where the electrons were orbiting the nucleus. And there was an understanding that moving charges radiated light - this was post-Maxwell, surely. Better go revise that history. So the upshot I guess would be that, anyway, there was a finding that the lines of light - oh also, the photoelectric effect which predicts that light are particles and have energy proportional to their wavelength, hey. So, this is how people worked out the energy gaps between the internal states of atoms that were later found to be related to inverse ratios of square integers: That led to the positing of a classical model, with a 1/r potential, that was inspired by the knowledge that

potential energy fell off like $1/r^2$. But did we get this backwards? Would have to revise the classical mechanics too, yikes. But yeah. The wise thing to do would be to talk angular momentum, and then from spectra we introduce Planck's idea of supposing that it *comes in units*. And then we add in the postulate of de broglie - where was this first verified? - and the double slit experiment, then the whole world turns just about on its head. And so was born the old quantum theory. Or something like that, go read Born and that Disney book for starters. Modern QM, QFT? Presumably there will need to be some historical preamble, but the idea is now that we lay out the foundational pieces of quantum theory as we now understand it, or at least as it will be used in this thesis. This includes, and perhaps is motivated by an example, leading to a small exegesis of the thesis Hilbert spaces and quantum states Probability amplitudes Operators and observables Time evolution Composite systems Density matrices Interactions Correlations & Entanglement And a survey of the present state: Formulation of QED Lamb shift, Rydberg constant, etc etc? Extension to QFT Experimental successes Extension to condensed matter What's after the standard model? Unifying HEP/condensed matter/QI? Following the math doesn't seem to have worked for SUSY (and so one might take this as a cautionary tale for Everrett).

Quantum technology is a young term, but has been growing exponentially since used in print for the first time in about 1970 according to Google Ngram. Some have said that we live in the 'silicon age', in light of the pervasiveness of computing technology based on silicon substrates. What is perhaps less conventionally appreciated is that modern semiconductor technologies, including the transistor which is essential to the miniaturized computing devices available today, are a direct outcome of the first quantum revolution - that is, the conception of quantum mechanics and its associated ontological metamorphosis. Understanding gained since the conception of QM has led to myriad other technologies that foundationally depend on the quantum world. Nuclear magnetic resonance, for example, underpins the life-altering technology of magnetic resonance imaging and finds use in the study of biomolecular structure and industrial applications, forming multibillion dollar industries. A second prominent example is the laser, whose functioning depends on the quantum theory of light and matter. Of course, lasers will be extensively used through this thesis for the purposes of preparing and investigating ultracold samples of Helium, but outside of the atomic physics laboratory lasers are now used in fields as diverse as electromagnetic and gravitational astronomy, medicine, self-driving vehicles and robotics, cosmetics, manufacturing, remote sensing, and miltary use. Despite their foundational reliance on the quantum picture of the world, these technolgies may one day be seen as 'primitive' in the same way that a typewriter or vacuum tube is now. A second quantum revolution began with the creation and manipulation of single quantum states, for which Haroche and Wineland were awarede a Nobel, but includes technologies such as ion traps and coherent control mechanisms, and the still nascent technolgies of single-system state determination. These are still developing but have laid the foundations for the third quantum revolution, the large-scale engineering of quantum states by

controllable interactions between multiple subsystems. The posterchild for such technologies is, of course, quantum computing. Notwithstanding ongoing controversy over the viability and usefulness of quantum computing, the challenge of large-scale quantum engineering has spurred an explosion of technical developments. Moreover, the growing prominence of quantum technology has drawn the curious eyes of computer scientists, who now join forces with physicists in attempts to unravel the basic structure of the cosmos from process-theoretic perspectives. Why is it, for example, so difficult to efficiently simulate quantum processes? Where is the border between efficient and intractable? The proof of genuine quantum advantages in certain processes may be one of the most profound statements about the nature of reality of this generation. Wherefore the nature of this advantage? Perhaps we will know before the century is out - perhaps, if ongoing crises arenot addressed - we will never know, and the cosmos may miss its chance to delve most deeply into its own self-awareness.

Digressions aside, a parallel stream of large-scale quantum engineering exists not in silico but in vacuo. The techniques of laser cooling to quantum degeneracy, established at the turn of the millenium, make quantum coherence (a topic to return to later) readily available and amenable to almost routine study. In the early days, cold gases were fantastic resources for studying atomic structure and basic interactions such as dimerization, because their low kinetic energies and densities dramaticall reduced the homogenous broadening effects that spectroscopy would otherwise be susceptible to. The development of advanced atomic clocks was a logical extension. In the later 90s though, Jaksch and Zoller proposed quantum simulation in optical lattices. Lattices themselves had been used before for some studies - check out Orzel for the work that *almost* got to the quantum phase transition - but yeah. That field is exploding now, with advances into microscopy and stuff.

Both of these topics - metrology and many body physics - form the spine of this dissertation. Also known as - internal structure and interactions - precision measurement and quantum engineering - stuff like this.

Ultracold atoms A brief history Cooling and trapping - who, when, why? BEC - a complete surprise and experimental triumph

Ultracold metrology Ultracold many-body physics

Democ

Why vacuum?

Physical models often make simplifying assumptions, like ignoring air resistance or friction, or collisions etc. Idealized models are only solvable in certain special cases, and introducing nonlinear effects like friction can make them mathematically intractable. This is partially resolved by sophisticated modelling these days, but the approximations will always remain. So when it came to studying microscopic systems, one would like to remove the background. so that the thing you are examining becomes not only the foreground, but the only thing in the image, and so your signal is not obfuscated. So people have tried to make vacuum for quite some time! Indeed this is one way atmospheric pressure was measured - Lavoisier used pumps from teh fire station to evacuate a chamber, and since then vacuum has advanced considerably.

Vacuum manufacture is a massive industry now, and I wonder if I could find a history of vacuum pressures over time to track the best known vacua. In the case of ultracold atoms, one needs to maintain a vacuum because the forces that hold the atoms in their optical or magnetic traps are so frail that capturing particles from the atmosphere would be all but impossible - what fraction would have sufficiently low energy to capture, and how long would they last? So, yeah, yuo need vacuum, and the lighter your atoms, the more worried you should be about vacuum. It also provided benefits like making sure lines stay narrow to mitigate pressure broadening et cetera - trapping atoms in vacuum is in some sense the ideal tool for the physicist - to study things in almost perfect isolation, to extricate the subject of study with complete mastery over its environment. But nature abhors a vacuum, and so will find ways to ruin your day. So there are a ton of ways to get a chamber close to empty. Let's talk about a few of them. Chamber architectures Scales Best vacua Mean free path & collision time

Cooling and trapping

Optical methods & limits In this section I give a hueristic introduction to laser cooling. The detailed theory of atom-light interactions will be saved until the chapter on atomic transitions where the theory becomes necessary to understand the work. If the next couple of secgtions aren;t sat leatst.

Consider a two level atom. It is probably possible to get away without using the word hamiltonian, so I would give a basic picture. Atoms can be thought aof as having two states: One where the electron is further away from the nuclers? state (as the sxcited state0) and that the energy level flips up or down with the adition of a photo. Oh ok so I would have to say why it is quantized perhaps, so there would be something to draw on in the chatper perfio previously, where I talk history of QM, which would probably include something about Planck's u idea of quantized areas phase space. But then again - there could well be a QM primer in the Moern er modern QM chapter - perhaps with the flag that 'this is the only math in the introduction chapter' but then there are things like the doppler cooling et cetera. I think perhaps a differnt structure would suffice: a non-technical summary at the top of each section/cahpter we with a digression into deeper and depper detail as you get towards the next section. Then people can tap out and push on to the next section whe Magnetic traps & evaporative cooling

The Doppler limit means that, for Helium, optical cooling to the ground state is not possible. This is when the velocity selectivity of the cooling light matches the velocity width of the sample. To reach the condensation threshold at the recoil limit, how big or dense would your trap have to be? Not reliable. This threshold was the limit for cold atom experiments until the development of evaporative cooling and polarization gradient cooling, which enabled the first production of bose-einstein condensates and resulted in the awarding of the 2001 Nobel prize in physics. Polarization gradient cooling is unavailable in Helium-4 because the spinless nucleus means there is no hyperfine structure, but fortunately evaporative cooling can achieve the low temperatures required for condensation in experimentally feasible traps. See any number of cold atom textbooks for an introduction or Ketterle's paper for a great

deal of detail. Here we provide a summary explanation only. Additional details are discussed in chapter 3, where the evaporative cooling process is part of the relevant experimental method.

Absolute limits of cooling Thermodynamic limits Third law & quantum proof Trap losses Modern methods Cooling fermions Prospects for feedback cooling? Quantized refrigerators Algorithmic cooling Other techniques: dilution fridges etc

Degenerate matter In this secion I will try to gvie a description of ultracold degnerate matter that even py a parents can understand! What a challenge. So I think it will be done in a cuple of parts. oNe where one considered a parabolic bucket with atoms rolling aroudn in it - at high energy they don't see each other. As they lose energy they get closer and clsoer to each other eeventually such that their interactions cant be ignored - they keep pinging off each other. They won't let the other balls take up ther space they are occupying. But there are two kinds of matter hey, there are bosons and fermoins. So at this pojt one would be able to intotduce the communtation relations in the technical part but fur the moment just accept: There is a wave-particle duality, you can see it with photon.s That would be a find introduction - well I guess it lives up in the itnro about when QM was born and all that. The double slit experiment would be a great example 0 maybe actualyl just the single slit, you know, that illustrates the diea of diffraction (does it?) and particles - depends what one is trying to show. I think yes the doule slit ecnompasses most of quantum (except entanglement lel) but hey. So yeah, I guess in this part would be something like a toy model, and then one can introduce the critical points like: That there is a ground state of traps, that the numbe rof particles in this state can be more than one when yuo are working with bosons, but not fermions. ANd they ahve to be cold - heuristically the picture could be that (because trying to avoid this idea of microstates) actually don't avoid them, but I really wonder how simple ane xplanation one can make here. But then again what's the idea behind going for simple? The're is the idea that someone will bea ble to read the thsis as a motivatedd undergrad, or as my parents so they sort of would be able to see what happened, or to new students in the lab, who could be able to read quickly but hey if you get to the point of joining th lab you must pbe pretty math-savvy. So. Yeah. What do we talk about? History of degenerate matter: Well that was sorta covered in the super intro.

Ok. Revising the content of this section. It will be the brief introduction to BEC. Consider a gas of non-interacting bosons in a harmonic oscillator potential. This can be treated in the grand canonical ensemble - plz clarify what the reservoir is - and so do you need to talk density matrix? I mean the Penrose-Onsager criterion is one way to do it. Seems relativistically fine - all good for the ground state biz but extends to nonzero momenta (moving frames). Blah. Bose-Einstein statistics. Bose enhancement re: scattering into the ground state. Point to references. Blah. No more words arriving. Let's fuck it I will see if I can get some formatting done here...

BEC three ways

The title is an illusion to Prithvi and my sketchy plan for pear, three ways. First,

the heuristic.

While the industry of European statistical physics was in its infancy, a young admirer of Einstein began asking questions would plant the seed of a flurry of work culminating in a technical triumph over the next seven decades. Satyendra Nath Bose made postulates about distinguishability - and noticed that such particles had dramatically fewer distinguishable microstates than they would if they were distinguishable. This, of course, has dramatic consequences for the statistical physics of systems constituted of these particles, which are now known as Bosons in his honour. Among the predictions that follow from postulating the indistinguishability of particles is that in the low-temperature limit, the velocity distribution diverges from the more familiar maxwell-boltzmann distribution. The threshold here can be thought of as the point where the intrinsic wavelike nature of particles becomes pronounced enough that the wavepackets of neighbouring particles begin to overlap, heralding a regime where the particle picture breaks down. Explicitly, Louis de Broglie's postulated that the relationship of momentum and wavelength of photons, $\lambda_{dB} = h/p$, was exactly true for all particles. The reason we do not see particles interfere at everyday scales is that the so-called de Broglie wavelegth is smaller than the particles themselves. Taken in concert with the equipartition theorem, one can assign the (mean?) de Broglie wavelength of particles in a gas of temperature T,

and in three dimensions one can therefore ascribe a the particles a'quantum volume' of λ_T^3. For a gas of density n, the volume per particle is $1/n$. From this argument, the quantum nature of gas particles cannot be ignored when $\lambda_T^3 \approx 1/n$, or when $n\lambda_T^3 \approx 1$. The latter quantity is called the phase space density, referring to the concentration of the likely atomic states into a small region of phase space, consisting of the position-momentum conjugate variables (footnote: Phase space is not just x/p but could refer to any set of conjugate variables, mathematically speaking). Below this point, the distinguishability of particles becomes crucially important.

In the case of indistinguishable particles, at a given temperature the probability that a single particle will occupy a given state of energy E is given by the Bose-Einstein distribution. Another way to read this is the number of particles that occupy a given state, on average, is given by the BE statistics. Remarkably, as the temperature vanishes, the population of particles falls overwhelmingly into the lowest-energy state. The temperature at which a macroscopic fraction of the atoms occupy the ground state simultaneously is called the critical temperature, and coincides with the temperature given above. This heralds the phase transition from a 'normal' gas to quantum degenerate matter, or Bose-Einstein condensation.

More formally, the critical temperature depends on the spectrum of the Hamiltonian, which must have a local minimum to allow for bound states. In this thesis, all experiments are performed in a magnetic trap which is described by a harmonic oscillator potential

$V = \sum_i \frac{m\omega_{x_i} x_i^2}{2}$

for which the critical temperature for condensation is $k_B T_c = \hbar\omega ho = (N/\zeta(3))^{1/3} =$

$0.94\hbar\omega_{ho}N^{1/3}$, where $\omega_{ho} = (\omega_x\omega_y\omega_z)^{1/3}$ is the geometric oscillator frequency and ζ is the Riemann zeta function. The fraction of particles in the ground state, or the condnesate fraction, is given by

$\frac{N_0}{N} = 1 - \left(\frac{T}{T_c}\right)^3$

when the gas is below the critical temperature. For the traps used in experiments in this thesis, the critical temperature is VERY LOW and the temperatures we reach are generally EVEN LOWER, producing condensate fractions about 95 per cent.

Condensation is a bona fide phase transition. The associated order parameter is sometimes known as the *mean field* and is defined as a complex parameter $\sqrt{n_0(r)}e^{i\theta(r)}$, where n and θ are the (potentially inhomogenous) ground state density and local phase of the macroscopic wavefunction. The imaginary part of the order parameter is nonzero probably because of stimulated scattering or something, so you wind up with constructively interfering particles. I guess. Either way, in this sense the BEC displays coherence at macroscopic scales - admittedly most condensates are only a few tens of microns across, but during our experiments they expand in freefall to an ellipsoidal volume of XXX - I wonder what the largest coherent volume is otherwise? How big is the biggest superconductor? Hm, I guess the magnets at CERN have us beat.

Macroscopic coherence is also manifest as off-diagonal long range order in the density matrix, as described by Penrose and Onsager (and leading to their definition of condensation in terms of the eigenvalues of the density matrix), and also has close analogies with Glauber's theory of optical coherence. Glauber's theory was extended by Sudarshan (?) to matter waves, which are distinct from the photonic case by ???. The theory of coherence makes predictions about the arrival-time correlations and distinguishes the g(2) function of the condensate (FUNCTION) from the thermal state (FUNCTION). These predictions were borne out by early experiments with metastable Helium, conducted in this laboratory using the same machine described in this thesis. For these reasons, the BEC is often referred to as a coherent state of matter, and the resulting pulses of atomic matter waves are called atom lasers in analogy with the coherent light sources, or lasers.

This, along with the various analogies between the optical propagator (the Huygens' equation) and the quantum mechanical one (the Schrodinger equation?), especially in the advent of techniques for reflection and dispersion of the momentum of coherent matter waves, led to the emergence of the term *atom optics*, and heralded a slew of experiments with matter waves that demonstrated the equivalence of optical and atomic systems, including matter wave interferometers and foundational experiments like Wheeler's delayed choice experiment. A distinguishing feature of atoms from light is that the atoms have intrinsic rest mass, and hence interact with each other gravitationally. This is the root of ongoing experimental campaigns to harness this distinguishing feature for applications such as gravimetry, and also to probe the interface of quantum mechanics and gravity, a central outstanding problem in modern physics.

1.3 Diagnostics & detection

Fluorescence Theory, some example plots Why the extension of lifetime? Off-resonant scattering rate lowered eh, plot curve vs wavelength? Calculation of population from signal Precision Absorption imaging Theory Sure, it's a momentum measurement, but let's calculate its limits Limited resolution and sensitivity - make some reasonable assumptions There is also fluorescence imaging in gas microscopes but we don't have the optics for this Delay-line detector System diagram Resolution in TXY Field of view in K-space Optics analogy Dark counts Saturation Atom lasers: CW, Pulsed & trap freq CW Sweep model temperature fitting? Correlations? Pulsed Outcoupling spectra Fourier broadening BCR 'Weak' number measurements & single-shot precision Trap frequency measurements Compressed sensing Aliasing Optimal sampling methods?

ECDL System diagram How dither locking works Experiment insertion Lattice build described in lattice chapter, stick to downstairs architecture to begin with TiS Seed & pump for 532nm TiSaf Cavity, crystal, etalon Locking system Doubler Mechanism Locking Calibration Software lock loop MATLAB architecture - appendix? Wavemeter How it works Cs crossover transition PMT setup - dither lock Stability of lock Bounds on accuracy of calibration Monitoring AI importing, intensity & SFP checks, WM lock check... Camera/mirror setup Reproducibility issues

Part II

Metrology

Chapter 2

Concepts in precision atomic spectroscopy

2.1 Light and matter

Find old notebooks for polarization writeup Read Rengelink thesis in detail

- Dipole response - fourier transforms, moments, correlations, line profile/impulse response...
- Spectroscopic notation - levels, intervals, orbitals, clebsch-gordan coefficients, origin of spectroscopic notation?
- Atomic structure calculations, QED, scaling of QED effects, opportunities in Helium?
- Polarization of light
- Jones and Stokes calculus
- Waveplates
- Transitions and selection rules
- 2LS, 3LS models
- Atomic polarizability

2.2 Trends in Helium spectroscopy

Metrology may be reasonably defined as the art of measurement.

The advancing precision of modern atomic spectroscopy is beginning to afford optical tests of fundamental physics in helium through, for instance, nuclear charge radii determinations. Helium now provides a testbed as appealing as Hydrogen for spectroscopic tests of QED and determinations of physical constants.

Early uses of spectra Discovery of Helium? Types of spectroscopy Emission & absorption spectroscopy State of the art methods Landmark results Lamb shift proton radius

Arguably, spectroscopy is the mother of all our understanding of matter. From spectroscopy was born quantum theory, spin, and the prediction of antimatter in relativistic quantum electrodynamics. But for all its triumphs, our best physical theory, quantum electrodynamics, falls short in some high-precision instances. For example, if you switch the electron in Hydrogen for a Muon and measure the respective Lamb shifts, you can determine the radius of the proton and find that it's different in each case. We need more measurements to constrain or discard competing theories. Fortunately, the simplicity of Helium allows predictions of its transition lines to some parts per trillion, accurate enough to compete with modern spectroscopy.

Quantum Electrodynamics, or QED, describes the interaction of charged particles with the electromagnetic field, whose fundamental excitations are identified with the more familiar photons, or particles of light. QED therefore describes the physics that governs all we see with our eyes, the interatomic forces from which arise the various familiar phases of matter, prevent solids from passing through one another, almost all technology (even nuclear physicists use electronic control and diagonistic technology), and indeed the dynamics of the action potentials in neurons. Hence, the purview of QED may well include the physics underlying the most intriguing of phenomena, perception. The detailed connection between quantum field theory and subjective self-awareness are beyond the scope of this thesis. For decades, quantum electrodynamics has stood unchallenged as the most accurate quantitative description of the world to date. Among its triumps include the prediction of the Rydberg constant to absurd precision and the correct prediction of the existence of antimatter. As the first synthesis of special relativity and quantum mechanics, QED laid foundations for more general quantum field theories, ultimately leading us to the standard model of particle physics. Undoubtedly, QED is a foundation stone in one of the great pillars of our understanding of the cosmos. However, as any sensible applied scientist will tell you: All models are wrong. QED, and QFT in general, presently has no formulation that is consistent with general relativity (other than in string theory, which despite its ambition and elegance has yet to satisfy experimental physicists). However, until we have the technology to synthesize black holes or other extreme gravitational conditions, we may not have experimental access to the high energy densities required to probe the Planck scale where quantum and gravitational effects are expected to be of comparable magnitude. Fortunately, we may not have to wait so long: The infamous proton radius puzzle, regarding the disagreement between experimental determinations of the proton charge radius, remains unresolved. Further, there remain statistically significant disagreements between predicted and measured energy levels in Helium. If there is an identifiable bias in theoretical predictions then, optimistically, one may find a legitimate need for physics beyond the standard model to explain these results. Therefore, experimental atomic physicists may find themselves prospectors for the fundamental discovery of the century. The experiments

described in the following two chapters constitute searches for evidence to constrain the search space of theories that purport to resolve the ongoing disagreements. Before describing the aims, findings, and methods of the experiments, I will provide a short refresher on atomic theory, terminology, and notation that is relevant to the following results.

Chapter 3

Measurement of excited-state and forbidden transitions in ^{4}He

- Paper: Tidy up future directions.
- Paper: Cite proton radius puzzle papers esp Wim's group
- Ensure existing segments fairly complete and flow alright.
- What sources of lorentzian broadening exist? Or narrowing?!

  * Dipole operator -¿ Clebsch-Gordan again

  This comes from the atom in an oscillating electric field. The Hamiltonian is where α and ω denote the Hilbert spaces of the atom and of the bosonic field, respectively, and $H_\int$ is the interaction term. In the plane wave picture, we can think of the electromagnetic field, with modes ω, then a *coherent* field has several connotations and implications.

  Classically, we can also describe the electromagnetic field as a vector field $E \times X$ with $E(x) : (x, y, z, t) \rightarrow \mathcal{S}(\S)$, where $S(x)$ is the Stokes vector at each point.

This chapter describes two measurement campaigns of electronic transition energies in Helium. First, I recount the method and used to measure the energy splittings between the 2^3P_2 state and a collection of states in the $n = 5$ manifold, including the first observation of a transition between the 2^3P and 5^1D manifolds in Helium. Second, I describe two methods used to measure the energy and the transition lifetime of the forbidden $2^3S_2 \rightarrow 3^3S_1$ transition, the weakest electronic transition observed in a neutral atom to date, previously considered too weak to be measured[**Lach01**].

The work described in this chapter provided the basis for the following publications:

- K. F. Thomas, J. A. Ross, B. M. Henson, D. K. Shin, K. G. H. Baldwin, S. S. Hodgman, and A. G. Truscott, Direct Measurement of the Forbidden $2^3S_1 \rightarrow 3^3S_1$ Atomic Transition in Helium, *Journal* **issue**(2020), ¡arXiv¿
- J. A. Ross, K. F. Thomas, B. M. Henson, D. Cocks, S. S. Hodgman, K. G. H. Baldwin, and A. G. Truscott, Measurement of spin-forbidden excited-state transitions in metastable helium, *Journal*, **issue** (2020)

3.1 Measurement of five $2^3P_2 \rightarrow 5L$ transition energies

Some of the $2^3P_2 \rightarrow 5_D$ transitions were observed by Martin in 1960[**Martin60**], but his measurements are in stark disagreement with present predictions[**Wiese09**] by about 13 GHzWhat about the other lines he measured? Were they all systematically off?. Further, in the NIST database, the transition energies to the 5^3D states are all identicalİndeed, in Martin's original paper, he only quotes measurements from 2^3P to the $5D$ level in general, indicating that his equipment did not have the resolving power to distinguish the fine structure of the 5^3D state. Martin was also unable to distinguish transitions to the 5^1D level, probably due to its proximity to the 5^3D lines Did he find similar transition strengths, or is this also a factor?. The contents of this chapter are complementary to the following publications:

3.1.1 Tests of fundamental physics with helium spectroscopy

Quantum electrodynamics (QED) describes the interaction of light and matter. It is the most accurate quantitative physical theory to date. The state of the art of experimental atomic spectroscopy is sufficient to match theoretical uncertainties in table-scale experiments, signalling an era in which atomic physics laboratories can contribute to tests of fundamental physics. Atomic structure predictions are made using the theory of QED and assuming the CODATA values of the fundamental constants. With the present accuracy of theory and experiment, it is possible to back-calculate from observed data and constrain fundamental constants. Schwartz identified opportunity to determine the fine structure constant in Helium in 1964, noting that the 2^3P fine structure intervals are subject to strong QED effects, but have lifetimes about an order of magnitude larger than the same states in Hydrogen.

The ongoing theoretical campaign [**Pachucki15**, **Pachucki17**, **Pachucki11**, **Pachucki10**, **Morton12**, **Morton06**, **Patkos16**, **Patkos17**] has reached sufficient accuracy to obtain a 4σ discrepancy for the squared charge radii difference between Helium-3 and Helium-4 obtained from the $2^3S_1 \rightarrow 2^3P$ and the $2^3S_1 \rightarrow 2^1S_0$ transitions[**Pachucki15**].

A comprehensive tabulation of Helium levels and transition rates was compiled by Wiese and Fuhr in 2009 [**Wiese09**], based on the extensive work by Pachucki, Yerokhin, Morton, Drake, and collaborators. These calculations were recently verified by Zhang et al [**Zhang15**]. Predictions are made using the theory of QED and assuming the CODATA values of the fundamental constants. With the present accuracy of theory and experiment, it is possible to back-calculate from observed data and constrain fundamental constants.

The theoretical campaign [**Pachucki15**, **Pachucki17**, **Pachucki11**, **Pachucki10**, **Morton12**, **Morton06**, **Patkos16**, **Patkos17**], has reached order $\alpha^6 m^2/M$ in both singlet and triplet states states[**Patkos16**, **Patkos17**]. Efforts are ongoing to compute the α^7 contributions expected to allow determination of the Helium nuclear charge radius accurate to 1%[**Pachucki17**]. Already, there is sufficient accuracy to obtain a 4σ discrepancy between squared charge radii difference between Helium-3

and Helium-4 obtained from the $2^3S_1 \rightarrow 2^3P$ and the the $2^3S_1 \rightarrow 2^1S_0$ transitions in each, namely $\delta r^2 = 1.069(3)$ fm^2 and $\delta r^2 = 1.061(3)$ fm^2 for the former and $\delta r^2 = 1.027(11)$ fm^2 for the latter[**Pachucki15**]. With improved calculations of 2^3P splitting to 1.7kHz[**Pachucki17**], experimental precision is now the limiting factor in determining the isotope shift.

Cancio Pastor *et al.* used Helium spectroscopy to make the then-most accurate Lamb shift measurement in any atomic system[**Pastor04**]. Six years later, Smiciklas *et al.* measured the 2^3P fine structure splitting to sub-kilohertz precision, determining fine structure constant to 5ppb[**Smiciklas10**]. Measurement of the 2^3P-2^3S spacing to within 1.4kHz would determine the nuclear charge radius to below 0.1%, better than expected from the muonic helium Lamb shift[**Wienczek19**].

Recently Kato *et al* refined measurements of the $2^3P_2 \rightarrow 2^3P_1$ to 25Hz accuracy, which can constrain α to less than one ppb in conjunction with similarly accurate measurement of the $2^3P_1 \rightarrow 2^3P_0$ transition and QED corrections of order α^7 [**Kato18**]. Ongoing efforts [**Pachucki17**] to obtain these corrections will also allow determination of absolute nuclear charge radii accurate to better than 1%, complementary to ongoing investigation of the proton radius puzzle.

Curiously, measured transition energies from the $n = 2$ manifold to the 3D levels are about 1MHz larger than predicted. Assuming the usual $1/n^3$ scaling of QED effects, such an anomaly would imply a deviation of $10/n^3$ MHz in ionization energy for an arbitrary state, motivating further study of transitions between states from different shells [**Wienczek19**]. In this work, we measure five transitions from the 2^3P_2 state to the $n = 5$ level, improving on the precision of past measurements[**Martin60**] by order of magnitude. We resolve lines from the 2^3P_2 to the $5^3D_{0,1,2}$ states individually for the first time. We make the first observation of the spin-forbidden $2^3P_2 \rightarrow 5^1D_2$ transition in Helium. Future measurements with greater precision could assist efforts to resolve a 7.5σ disagreement between the predicted and observed $n = 3$ singlet-triplet splitting[**Morton06**].

3.1.2 Detection scheme

- Setup - alignment
- Procedure
- Mechanism
- Calibrations
- Analysis

Procedure

We use a micrometer translation mount on the final lens to align the beam on the Helium sample. We locate the transitions approximately by using the maximum

available laser power at the predicted frequency, and then reducing the power and adjusting the frequency set point until the signal no longer saturates at the peak. We then scan the set point of the laser across the transition to obtain the transition signal. The beam was initially aligned by tuning the probe beam to the predicted value of the 53S1 transition and operating with the maximum available power. Although the uncertainy in wavemeter accuracy was larger than the transition linewidth, by operating well above the saturation intensity, the transition was broaded by tens of MHz and so the WM error was less significant. When scanning the beam pointing across the expected target region, approximate alignment was signaled by a dramatic loss of atom number. When the signal saturated, the power was lowered until the signal was just above the noise floor, and then scanning resumed. This process iterated a few times until the maximum attainable signal was below saturation - that is, when for fixed power one could not completely destroy the trap. Notice there are three kinds of saturation here: Atomic population saturation, detector saturation, and signal saturation when you run out of atoms. perhaps the term 'dynamic range' would be more suited to the latter... Something to think about. Sequence diagram During the calibration shots, we also block the beam with a mirror mounted on an automatic translation mount. The profile and polarization of the beam are determined with lenses and waveplates prior to vacuum entry. The measurement sequence consists of measurement shots with each of the two magnetic field strengths followed by calibration shots, wherein the laser beam is blocked and switched off. We calibrate the wavemeter before each transition measurement. Analysis of the wavemeter stability suggests that calibration drift is not a significant source of error, as discussed in the supplementary materials.

The method therefore consists of alternating measurement trials with control trials, wherein the laser beam is blocked before the fibre coupler with a flipper mirror. At the moment I use an interpolation, but I might want to try using a model-based estimate of the atom number. Either way, there is going to be some error in the number estimation. It's probably small. The difference between the interpolated, unperturbed atom number and the detected number in the measurement trials is affected by the quantum efficiency and the introduced uncertainty in atom number.

The polarization of the light was fixed with the waveplates before the chamber. Can you tell handedness just by relative angle of waveplates? We hypothesized that the initial state of the atoms during the cooling phase was in the m=2 state, as the optics are configured to drive with a sigma+ beam during the in-trap cooling stage. I verified this by driving with plane-polarized light (in the atom frame - put some trap sim in to show where the field points), which is a linear combination of sigma+ and sigma- light. If there were atoms in initial states other than the m=2, then when driving to the 53S1 state, one would observe multiple peaks. Instead, only one peak was observed, which vanished when the probe beam was set to sigma+ light. (I think check the data).

The measurements are taken at two different background field strengths. Therefore the detuning from cooling resonance is X and Y MHz in each stage, respectively.

Line	Beam waist (cm)	Beam power (mW)	Peak intensity (W/m^2)	Exposure time (ms)
5^3S_1	4.1	2.73(1)	3.1(2)	100
5^3D_1	4.1	4.5(1)	5.2(1)	150
$5^3D_2, 3$	4.1	8.6(1)	9.9(1)	250
5^1D_2	0.1	10(2)	6.3E3	100

Table 3.1: Probe beam parameters

Stage	Beam power	AOM detuning	Peak intensity	Transition detuning

Table 3.2: Pump beam parameters

These values were calibrated independently by an RF spectroscopy technique. This allows empirical extrapolation to the field-free transition energy by correcting for the calculated Zeeman shift of the centre frequency of each measured line.

Data acquisition

This probably goes in the Intro/BEC machine part

Following the laser interrogation, the remaining atoms are gradually outcoupled from the trap with a pulsed atom laser. At the beginning of each shot, the LabView control interface writes a line to the log file with the parameters `timestamp, laser_setpt, shot_t` where `shot_type` is either `stage_1`, `stage_2`, or `calibration`. When importing the data into the processing scripts, the

As the laser set point is fixed for sets of three shots (one per field setting),

Mechanism of action

Do the damn modelling:, 2^3P population, 3level model, Evaporative cooling model, Estimate sensitivity to photon scatterings, Upper state lifetimes? To drive the transitions from the 23P2 state to the states in the n=5 manifold, I use the probe beam to disturb the near-resonant optical molasses cooling stage of the experiment. This follows the MOT loading and precedes evaporative cooling, and operates with XYZ beam parameters for XXX ms, and then with ABC beam parameters for YYY ms. I calculate that during these stages, the excited-state population is ZZZ per cent, which are then susceptible to scattering photons from the probe beam.

I used the evaporative cooling sequence as a transducer between scattering-induced heating of the cloud and the final condensed number. I will present a quantitative sketch of the mechanism below, but one can also take a heuristic understanding from the following argument:

The evaporative cooling we use to achieve Bose-Einstein condensation has stringent tolerances on initial phase space density, which increases with number and at lower temperatures. Tuning a radio chirp to the spin-flip transition from a trapped to an untrapped state and sweeping down to lower energies, higher-energy atoms are removed, the cloud rethermalizes at a lower temperature, and the phase space density

increases. Higher-energy atoms spend time further from the centre of a harmonic magnetic trap. So, scattering photons from the probe beam heat the cloud, leading widening the velocity distribution, which drives more of the atoms into resonance with the radio chirp. The final temperature is determined by the endpoint of the radio chirp. Resonance with the probe light manifests as a signal in a reduction of the final population of the condensate.

As I said, an essential part of our BEC production is an optical cooling and spin-polarizing stage which precedes the loading of our magnetic trap. This ensures a nice large atom number and low temperature. This give us a nice big phase space density, a dimensionless number which compares the length scale of quantum interference, the de Broglie wavelength, with the interparticle spacing given by the particle density n. So, disturbances to this initial condition by atom loss or heating will reduce the phase space density input to the evaporation stage. The Bose-Einstein condensation threshold occurs when the phase space density crosses about 2 - for comparison, atmosphere has a phase space density about one ten millionth of that. One can therefore think of the RF evaporation as a phase space amplifier in the following way:

Evaporative cooling works by creating a resonance between trapped and untrapped magnetic states of atoms with a specific Zeeman splitting by exposing the cloud to radio frequency radiation. Energetic atoms travel up the magnetic field gradient, shown by the thickness of the purple lines, to the ellipsoidal shell defined by a fixed field strength at which the atoms resonate with the radio waves. The atoms are then transferred into free states and leave the trap, taking with an amount of energy greater than the ensemble average. This basically cuts out the upper tail of the Maxwell-Boltzmann distribution, driving down the atom number, but also the temperature once the cloud rethermalizes. If you get this right, you continuously increase the phase space density by making the cloud cooler and smaller, until you get to BEC. The endpoint of the RF chirp fixes an upper bound to the energy of the trapped atoms, and hence a temperature. Then the phase space density can be estimated by counting the number of atoms you have left. We measure this atom number using Helium's unique detectability - by applying broadband radio pulses to the trap we free about 0.5% of the atoms at a time, creating a series of pulses of coherent matter waves, known as an atom laser. This resolves on our detector as a series of discrete particle detection events, which we sum up with an abacus. So by controlling our independent variable, the applied laser frequency, we have a gain mechanism that allows us to measure the dependent variable, which is the phase space density reduction by resonant scattering of photons from the probe beam.

Calibration measurements

After the probe is applied during the optical molasses cooling, we use a standard forced evaporative cooling procedure. At the end of the sequence the atoms are in the metastable 2^3S_1 state which exhibits a 19.8eV ground state separation. This internal energy enables single-atom detection by a multi-channel plate and delay-line

RF centre frequency	Calibrated field strength (G)	AOM frequency (MHz)	Detuning (MHz)
XXX	18	138	0.5
XXX	11	133.6	2

detector stack with an efficiency of 8 per cent[**Manning10**] to determine the atom number loss. We use a pulsed atom laser [**Manning10**, **Henson18**] to transfer atoms to the untrapped state and avoid detector saturation.

A translation mount on the final lens gives us micrometer precision in the placement of the focal point on the beam, which we use to align the beam on the trap, threading a ten micron needle in the dark 20 micro-radian accuracy.

Get data for AOM and RF calibration AO offsets 138MHz and 133.6MHz ? cooling transition is split 25.55 MHz, and 16.002 in stage 2 Therefore the beams are (ish) detuned 0.5 and 2MHz respectively

Analysis

In this section I describe the data processing method used for the peaks, using the 5^1D_2 line as an example.

3.1.3 Findings

Results

3.1.4 Determination of transition energies

We empirically extrapolate to the field-free transition energy by correcting for the Zeeman shift in the observed lines. The exposure time and intensity varied among measurements to avoid saturation.

The table below displays the results of the measurements, including predicted linewidths. In the case of the 23S1-33S1, the measured Einstein A coefficient is also listed. These measurements are accurate to a few hundred parts per billion, and their accuracy is limited by the absolute accuracy of the wavemeter we used as a reference for the laser lock. Within the accuracy stated by the manufacturer, these results are consistent with the predictions of QED. Of the six lines measured, three have been resolved individually for the first time, and two have not been recorded elsewhere. The centre frequencies are obtained by fitting Lorentzian profiles to the atom loss spectra. Have a look at residuals; what are the expected broadening effects? What are the expected systematic errors? Error budget goes here also.

Ah. The CG madness is only needed for the triplet D states. The singlet D and the triplet S have zero total angular momentum for the spin and orbital dof, respectively, so the basis is trivial and in these cases, we can use the linear extrapolation method with no worries. What about the 2 3P2? Oh - I missed a point, which is the presence of other nearby levels. For the singlet D, that's done, it's unique, as S=0. And for the triplet S, also, as L=0. Not so for the 2 3P2. But they're several GHz away so

$\|e\rangle$	$f_{\text{meas,1}}$	$f_{\text{meas,2}}$	$f_{\text{field-free}}$	Δ_{theory}	$\text{FWHM}_{\text{obs.}}$	$\text{FWHM}_{\text{pred.}}$
5^3S_1	727,303,223.89		727,303,249(5)	4.4	3.12(40)	9.21
	727,303,234.04					
5^3D_1	744,396,453.41		744,396,496(21)	-16	5.79(62)	16.4
	744,396,477.82					
5^3D_2	744,396,191.21	744,396,223.01	744,396,217(22)	-12	4.18(50)	16.4
	744,396,204.67	744,396,224.64				
5^3D_3	744,396,160.46	744,396,195.49	744,396,201(21)	-8.7	4.04(12)	16.4
	744,396,182.37	744,396,208.29				
5^1D_2	744,430,295.37		744,430,347(21)	2.5	3.21(13)	13.9
	744,430,316.37					

Table 3.3: Summary of results (all in MHz) For each transition. The measured frequencies are obtained in an ambient magnetic field of strength 18G (top row) and 11G (bottom row). After correcting for the AOM and vapor cell shifts we extract the centre frequencies f_{meas} from Lorentzian fits with statistical error at the 10kHz level. For the 5^3D_2 and 5^3D_3 states, each line shows the pair of transitions corresponding to the magnetic quantum number of the upper state $m_u = 1$ and $m_u = 2$, respectively. After correcting for Zeeman shifts, the field-free energies $f_{\text{field-free}}$ are obtained, and shown with statistical error in parentheses. We show the difference Δ_{theory} between our measurements theoretical predictions [**Drake07**]. Observed line widths are the mean full width at half maximum $\text{FWHM}_{\text{obs.}}$ of a Lorentzian fit to each line, with theoretical predictions $\text{FWHM}_{\text{pred.}}$ from [**Drake07**].

that shouldn't be a problem at all. Well, then that's cleared up! Great. Now to write this nonsense up. Start concise in the paper, then we can expand it here. later.

Figure 2 shows the spectra measured using this technique. Table I summarizes the results of our measurements. An account of our error budget is given in the supplementary materials, and summarized in Table II. While we are able to resolve the 5^3D_1 peak, the 5^3D_2 and 5^3D_3 resonance are sufficiently close together to cause significant quantum interference effects [**Marsman15**], and require special treatment to obtain the zero-field values.

Error budget

The statistical error in the centre frequency of our Lorentzian fits is less than a MHz, fixing these transitions to some parts per billion, with MHz differences from theory. The last measurement of the $2^{3\text{P-}5}3\text{D}$ gap could not resolve the fine structure splitting, about 300MHz, but we resolve them with excellent visibility. To give credit where credit is due, the last measurement of these transitions used a discharge cell submerged in liquid nitrogen, passed through a window to an in-vacuum diffraction grating and illuminating a phosphor screen with lines whose splitting was measured with a ruler against a Mercury reference. Still, they were wrong.

But, our ultimate accuracy is limited by the wavemeter to 20MHz in the worst case, or 4MHz when close enough to the calibration line. Unfortunately, we don't have the precision required to compete with the state of the art, but had we a frequency comb reference then we'd be in the game for tests of fundamental physics. Still, we correct

the previous values by thirteen gigahertz, update four values in the NIST database, and add a new line to boot. We conclude that within our experimental uncertainty, QED is correct.

The AC Stark effect from the probe beam varies between the measurements, but in all cases is calculated to be less than 1MHz, in agreement with an empirical determination described in the supplementary materials. The recoil shift is ambiguous in sign because of the counterpropagating pump beams, but the shift is at least an order of magnitude less than the absorption linewidth.

Source	Shift (MHz)	Unc. (MHz)
AC Stark (Pump)	<0.1	-
AC Stark (Probe)	<1	-
DC Stark	<0.1	-
Mean field	<0.1	-
Recoil	±0.218	1
Wavemeter	0	Variable
Doppler	XX	YY
Pump lock	N/A	0.3
Probe lock	-190MHz	0.1
Cs cell	-1.9	4
Total	-1.9	4.1+WM

Table 3.4: Error budget for the measured lines.

Discussion

We improve on previous measurements with an order of magnitude greater precision and report the first observation of the spin-forbidden $2^3P_2 \rightarrow 5^1D_2$ transition in Helium. Our measurements constrain the 5^3D and 5^1D ionization energies of ^{4}He to 150 parts per billion, and the 5^3S 5^3S to 28 parts per billion. The theoretical transition energies agree with the observed values within experimental error.

We performed multilevel laser absorption spectroscopy of excited states with ultracold atoms in hard vacuum. Our measurements agree with current predictions within our error budget. A 93σ difference between Martin's measurement[**Martin60**] and predictions [**Morton06**] of the $2^3P_2 \rightarrow 5^3S_1$ and $2^3P_2 \rightarrow 5^3D$ intervals are resolved by this work. Our measurements constrain the 5^3D and 5^1D ionization energies of 4He to 150 parts per billion, and the 5^3S to 28 parts per billion. This work provides four contributions to the NIST database of atomic spectral lines.

In Martin's original paper, he only quotes measurements from $2^3P_2 - 5D$, indicating that his equipment did not have the resolving power to distinguish the fine structure of the $5D$ state. Martin's measurements were made using a nitrogen-cooled Helium discharge lamp fed through an in-vacuum prism onto photographic plates where line separations were measured with a ruler.

The apparatus used for this experiment is presently being upgraded to operate with ^{3}He - ^{4}He mixtures. This technique could be employed, along with an improved

frequency reference such as a clock-stabilized frequency comb, to constrain the charge radius difference for comparison with other transitions.

What accuracy is required for charge radii differences?

3.2 Detection of the forbidden $2^3S_1 \rightarrow 3^3S_1$ transition

After our measurement of the 2P-5L transitions, our eyes turned to the 427nm transition. To our knowledge, nobody had measured it. We found that we required ten orders of magnitude greater sensitivity in order to detect this transition - a few mW over a few ms wasn't going to cut it. After discussion we decided that the most promising method might be to look for heating or loss by directly illuminating a BEC - having found previously that weak trap lifetimes can in fact be several minutes. However, before we embarked on the measurement, I performed some simple calculations to estimate the order of magnitude of the best signal-to-noise ratio we could expect.

We determined that this SNR would be sufficient to warrant making an attempt at the measurement.

RECOUNT CALCULATION * 3 level measurement * Clebsch-gordan coefficients and net transition rates * Collection efficiency monte carlo

For this measurement, the data processing methods were the similar to the 5L transitions - a drift model was created to predict the undisturbed atom number in a given shot, based on atom number measurements from the calibration shots. Wait - did the outcoupled fraction get used, counting the number dropped versus the number left in the trap? Were these things tried? Talk to Kieran.

This method allows for the extraction of the line centre and width, which determines the state lifetime. However, the state lifetime is dominated by a fast decay to the 3P state, the oscillator strength of which is many orders of magnitude larger. The oscillator strength - which is proportional to the Einstein A coefficient - of the transition can be obtained by another method, described in the next section.

We develop a second method to determine the Einstein A coefficient of the specific forbidden transition. We perform time-dependent thermometry of the a thermal cloud (above the critical temperature) while alternating shots with and without the probe beam blocked. During these sequences, we use RF pulses as per standard procedure (although in this case the term 'laser' is especially misleading as the source is incoherent) and fit a Gaussian profile to each pulse. During the 25 second hold time, the cloud heats at a rate of X K/sec. This is possibly due to: Penning ionization, magnetic field noise, background collisions, majorana leaks? How does it depend on number? Anyway. With the probe beam applied, the calculated scattering rate of up to Y Hz corresponds to a peak additional heating rate of Y J/sec.

We fit the time evolution of the temperature of the thermal cloud with a linear model and obtain the change in heating rate with respect to the probe-free shots. We can then back-calculate via the specific heat of a harmonically trapped Bose gas to

determine the energy transfer rate (which should just be proportional I think, when above the critical temperature?), hence the photon scattering rate. And so lo and behold we can determine the A coefficient, and look, it's really weak! What a great job we did. I wonder whether Kieran's method is a bit sketch because does heassume a certain density distribution??

Power & curvature measurements - what actually drives Quadrupole transitions?

3.2.1 Proof-of-feasibility calculation

3.2.2 Two detection methods

3.2.3 Findings

Error budget

Results

Isotope shifts & better reference Different target transitions?

https://physics.stackexchange.com/questions/430532/why-are-there-no-transitions-between-orthohelium-and-parahelium

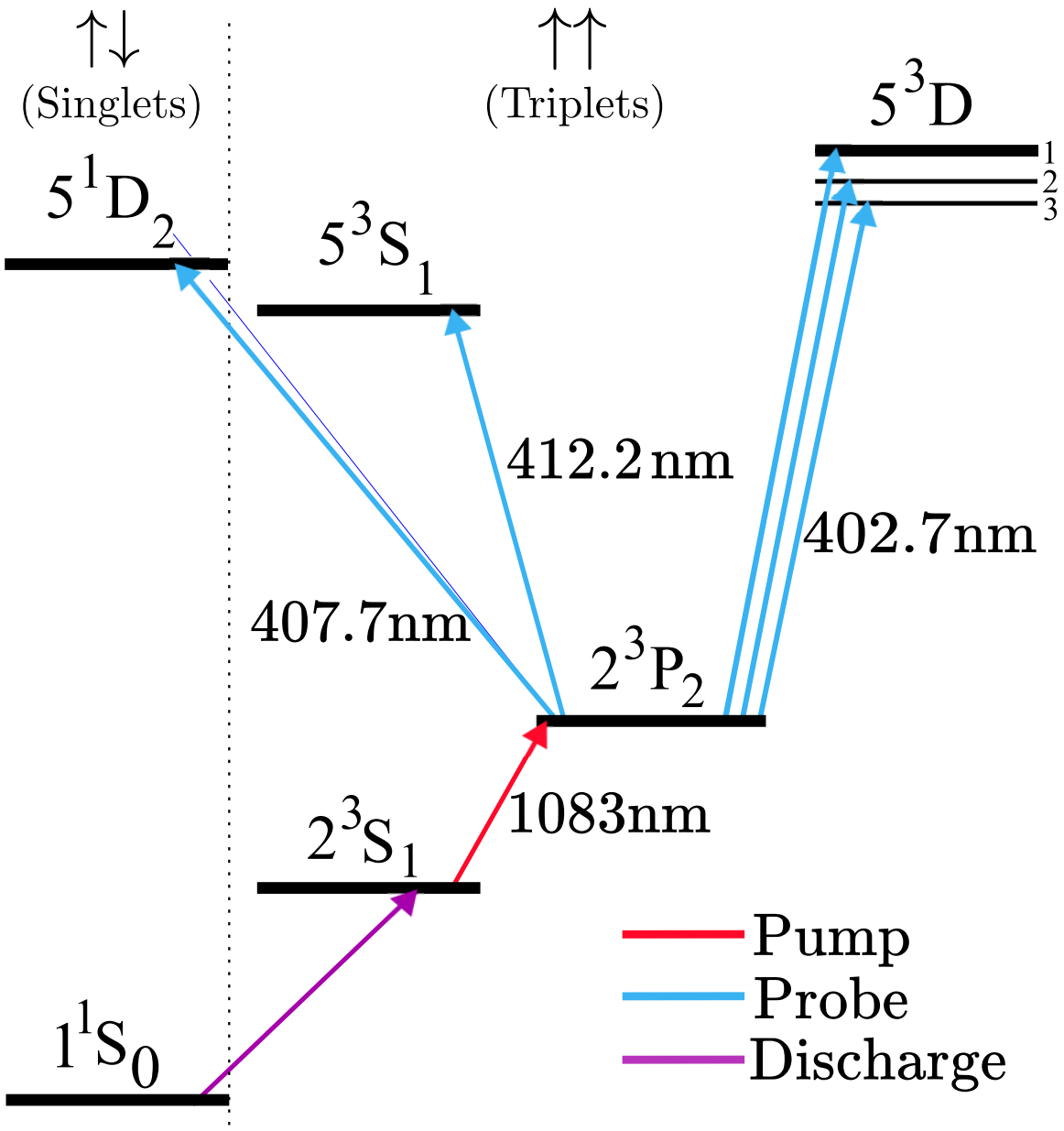

Figure 3.1: A level diagram for the helium atom. The transitions measured in this work (blue), are driven by a tunable laser referred to in text as the 'probe'. The cooling transition (red) is referred to as 'pump' throughout the paper and populates the lower state of the target transitions. The doubly forbidden $1^1S_0 \rightarrow 2^3S_1$ transition is excited in a high voltage discharge cell. Transitions between the singlet and triplet manifolds (left and right of dotted line) are forbidden in the dipole approximation. The level splittings are not to scale.

Figure 3.2: Measured line profiles for the $2^3P_2 \rightarrow 5^3S_1$ (left) and $2^3P_2 \rightarrow 5^3D_1$ (right) transitions, with Lorentzian fits. On the horizontal axis is the probe laser frequency ν, relative to the theoretical prediction for the magnetic field-free splitting. The vertical axis is the response as measured by atom number loss relative to the calibration shots. Theoretical predictions (vertical bars) are Zeeman shifted from the zero-field value according to the field calibration, with uncertainty (horizontal bars) dominated by uncertainty in background field strength. Lines obtained by measuring against an 18G and 11G background field are shown in red and blue, respectively.

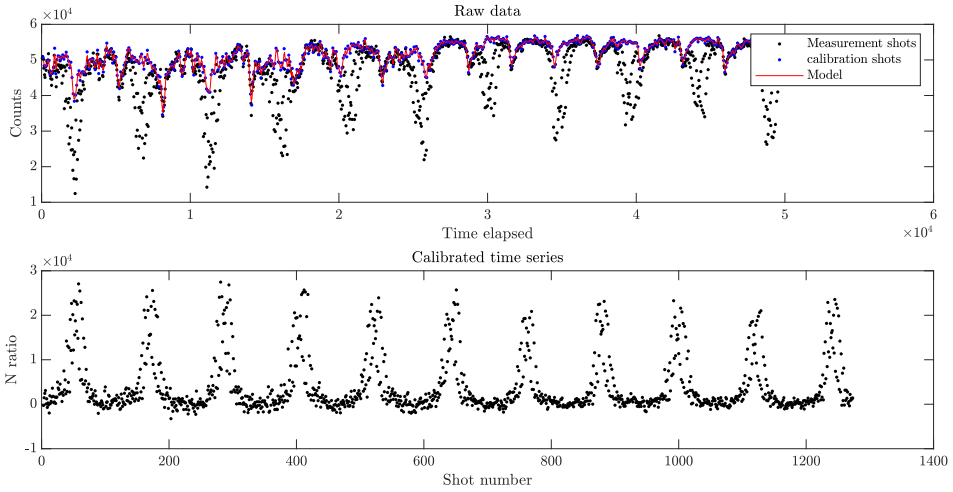

Figure 3.3

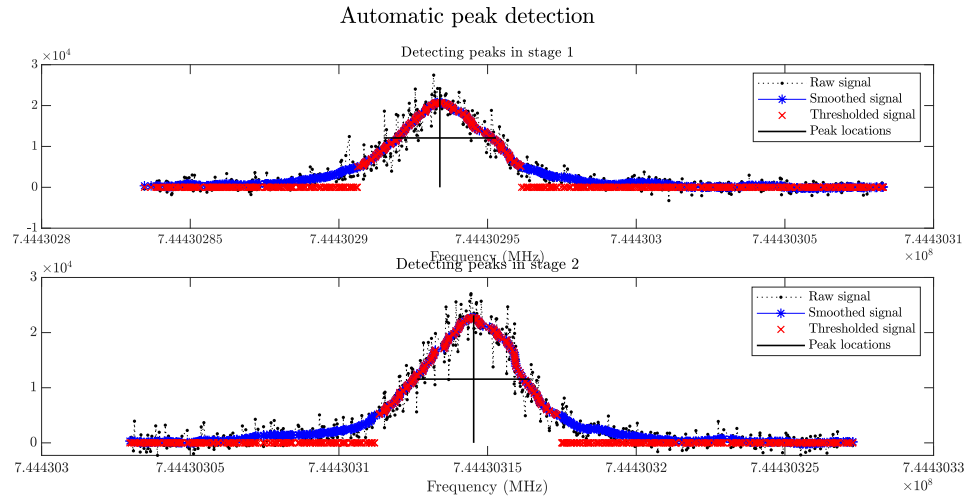

Figure 3.4

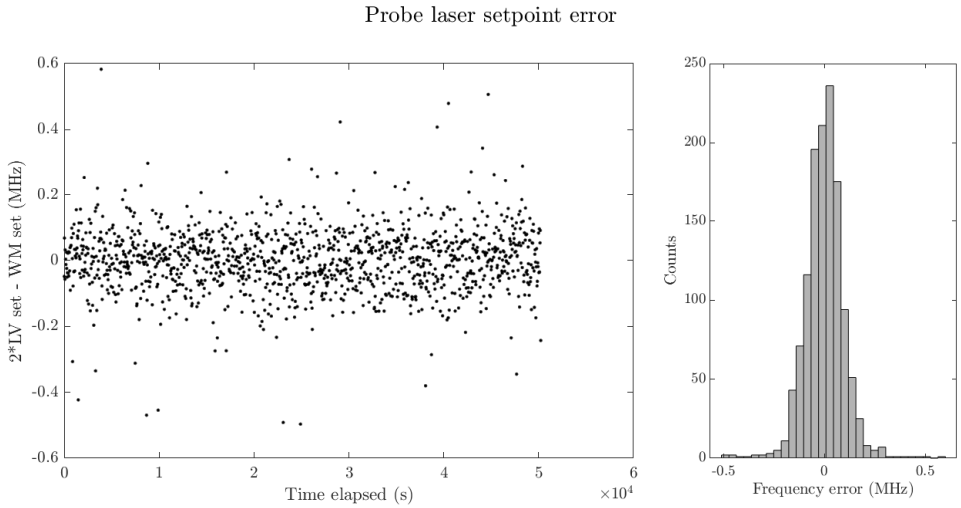

Figure 3.5

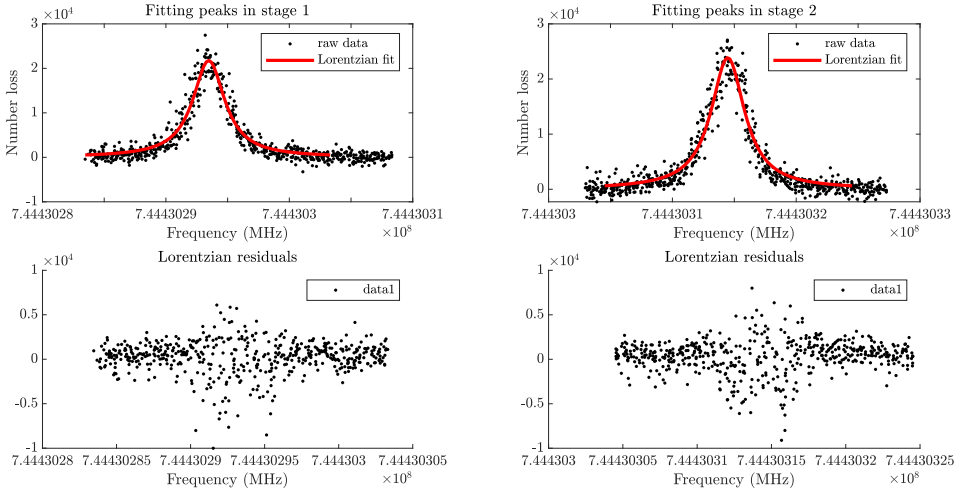

Figure 3.6

Figure 3.7: Line profile for the spin-forbidden $2^3P_2 \rightarrow 5^1D_2$ transition, presented similarly to figure **??**.

Figure 3.8: Line profiles for the $2^3P_2 \rightarrow 5^3D_2$ and $2^3P_2 \rightarrow 5^3D_3$ transitions, driven by a mixure of σ^- and π- polarized light and presented similarly to figure **??** and **??**. The large central peak is the overlap of two peaks, the transitions to the XXX and YYY lines, which are nearly degenerate for the entire operational range of our background magnetic field.

Chapter 4

Determination of the $2^3S_1 \rightarrow 2^3P/2^3P$ tune-out wavelength

4.1 Magic Zero

4.2 Measurement technique

4.2.1 Model of mechanism

4.2.2 Experimental implementation

Alignment

Laser polarization measurements

4.2.3 Data processing

4.3 Findings

4.3.1 Error budget

4.3.2 Results

Silence - nothingness - stillness. A subject of fascination for humans over centuries. Entire schools of meditation practise, and pursuits of divinity, seem to be pointed towards realizing perfect stillness. The space between the breaths. The stillness of the mind and the insights that follow - from simple clarity. The universe, however, is never motionless. Whatever zero-point energy happens to be - suggests that true stationarity is impossible. And likewise, in depletion, nothing can be truly empty, thanks to vacuum fluctuations. But there is the resounding theme throug thsi thesis, right of approaching the motionless, of approaching the definitive, the ability to say precisely waht something is. To distill an element of truth, and the effort it takes to wrest away so much of the noise of the world is titanic. The continual drive to split the subject from the object - by ensconcing it in vacuum, by isolating something

with laser precision, a *pure* sample in *stable* conditions - in some sense perfectly well-defined, perfectly characterized, and perfectly frozen. But nothing in reality is so simple - even at the ground state, there is endless detail - field noise, et cetera.

The condensate aquiver in the ground state - depletion. As ketterle said 'exquisitely isolated' The interplay of internal structure aligning perfectly to isolate the atom from the world. THere's poetic beauty in this. There's an allure. But elusive, and so is the condensate - the QM description works but there are always going to be traces of the initial conditions, right?

So, tuneout.

Electronic transitions can be violent events! THe electron cloud completely reconfigures. A disturbance in the electric field, the energy ripping out from the cloud (go read the attoclock/electron tunnelling papers maybe) - we continue the journey down to weaker signals in pursuit of the measurement of nothing. That nothing is almost always impossible to measure - detector noise, for instance, always present, and the ever-pervasive background. Best we can do is to account for all these - but zero crossings are easier to meaure.

Blah. Even in TO we don't realize a state of perfect stillness - it's done by trying to shift a frequency. But to make it indistinguishable. We tried the trap driving method but that didn't really work.

Intuition: Classical oscillator Polarization & Polarizability Sketch of method Trap freq theory Nonlinearity & anharmonicity - why did our traps chirp? Model never quite nailed the same chirp did it? Was it trap ringing in the end? Uses of Tuneouts Previous measurement

Have TO been used for QED? Measure the TO with sufficient precision to test QED

We did it. Error budget.

Trap configuration

Alignment We employed three stages of successively increasing precision to align the probe beam with the magnetic trap, using a 2W? 532nm laser, followed by a 300mW 450nm beam, and finally using the tunable laser at approx 405nm?. The first beam was used for coarse alignment by scanning the vertical position of the focusing lens and dropping the BEC onto the phosphor detector. This technique has been used previously to align beams - reason being that the repulsive dipole potential of the 532nm beam creates a fissure in the BEC as the fallinc condensate diffracts around the beam. The effect is weak but visible as a dark stripe through the BEC - at least, ideally. Sadly, our ingenuity held us back (yet again). We used a pickoff plate - a large spherical optic which is weakly reflective at the target wavelength - for initial scans, deflecting a fraction of the beam onto a CCD (as described in the Laser System chapter). Unfortunately, Bryce dropped this optic at point point and the rim of the glass lost a chip. We did not notice for quite some time that this had altered the strain distribution on the transmitting surface of the optic, and actually completely destroyed the beam profile. How did we find this out, again? This led us to replace the optic with a mirror on a hinged mount, so we could remove the mirror

and return it to a controllable position. Once we removed the damaged optic, we were quite quickly able to find a signal in the disturbed BEC. I think we eventually used the atom laser for a better visible signal - although the phosphor had a better dynamic range, the brightness difference was hard to see by eye, but integrating over several PALs gave us a density profile we could use. We aligned the beam with the fall path of the condensate by ensuring the destruction was in the centre of the falling condensate, and then raising the beam step by step until the signal vanished. At this point we figured we'd overshot the trap, so stepped back down and changed to another beam after marking beam position on the CCD. We then changed to the high power 450nm beam because it would produce a strong polarization response in the condensed atoms. We then ran successive trap frequency measurements while adjusting the beam position, looking for disturbances in the oscillation frequency under the same mechanism by which our measurement method works. When this signal reached a maximum with respect to position, we iterated adjustments in lens position along the beam axis with adjustments in pointing (as imperfectly aligned optics would couple these degrees of freedom). When this signal was maximized, we switched to the probe beam at 405nm. At this wavelength the atomic polarizability is positive so the beam is attractive. We therefore adjusted the sequence by switching off the beam at XXX ms after the trap release. When the beam was aligned we observed a second peak in the detection rate (picture), from the release of atoms trapped in the beam. We iterated this alignment procedure until the number of trapped atoms saturated - assuming this to be pointing at the BEC. Then we switched to alternating shots measuring the trap frequency, as in our measurement method, and adjusted the lens configuration until the frequency difference between the measurement and reference shots reached a maximum. Then, because the optical dispersion would be such that the beam pointing and focus would vary with wavelength, we repeated this procedure after taking steps of a few nm at a time towards the tuneout wavelength, eventually settling within a few MHz of the transition on the assumption that a few ppb change in frequency wouldn't bother us. We measured the distance from the focus lens to the chamber centre with reference to a technical diagram, and positioned the CCD at this distance away from the focus lens (including the reflection off the alignment mirror) but of course the beam before the focus lens would not have been perfectly collimated which might have affected the outcome.

Tune-out for fixed polarization

As described in the section above, for fixed laser intensity, the polarizability of the atom in the neighbourhood of the tuneout is proportional to the detuning from the tuneout. We used the machine control interface to automatically iterate the laser setpoint in steps of XX MHz for total scan sizes of YY MHz about the Tuneout. Alternating shots between measurement and control, where the laser was blocked on the pre-fibre side (even though the AO could be set to zero, light leakage had been observed. Why? Probably the zero offset of the photodiode. And also leaking fundamental light? I mean, we characterized that anyhow, will have to dig up that measurement). We use the calibration shots to produce a drift model to predict the

underlying magnetic trap frequency (details?), then take the difference of squares of the measured frequency and the predicted frequency. Below is a plot of the squared difference versus wavelength for a single scan (PIC). The zero crossing is determined by fitting a linear model and solving for y=0. There was not a statistically significant quadratic contribution to the signal. The stat error in the zero determination is X. Sys contributions at this level are Y.

The gradient of the line was found to vary, and in some cases invert in sign. While initially puzzling, this turned out to be a useful validation of the trap frequency picture came from the inadvertent observation of a change of sign of the trap frequency change. This was eventually ascribed to the sign change in the second derivative of a Gaussian function, which shows that the small-amplitude oscillation picture described above is actually quite accurate despite all the approximations (like, how big is the BEC?). (PIC)

Polarization dependence

We measured the dependence on polarization by adjusting the waveplate optics. We took wide scans (several GHz) about the TO for a few WP values, and produced an empirical model to predict the frequency of the tuneout as a function of waveplate angles. This helped us search for appropriate scan regions as we iterated. We did not rely purely on predictions based on waveplate configs as the birefringence would have been wavelength dependent (and we were about a nm from the spec wavelength - estimated error here? These are zero-order, so could perhaps estimate this, assuming no change in refractive index, just from the physical size diff maybe...). Not to mention there was the unfortunate fact that we put the focus lenses and mirrors after the optics - will be a tricky thing to put into the thesis, how we screwed this up and spent so long trying to correct it...

As we have numerous scans across the tuneout in any given run, we have some options for processing. One would be to bin the shots by set wavelength, and fit the average values. However, this would lead to issues with trap frequency or alignment drift? But the solution we took was to determine the zero crossing each scan separately, then take an average over a given run weighted inversely by the statistical error in that shot. This is because deviations from perfet alignment would manifest as a lower gradient and hence reduced sensitivity - so did the gradient or the stat error get used as the weighting function? Should go check. This introduced a stat/sys error in the fixed-polarization tuneout of XXX MHz.

We did not, in the end, know what the final state of the polarization was. We used a beamsplitter to measure the min/max transmitted power as a function of QWP angles (go revise the method) to determine the degree of linear polarization, leaving the sign of the circular component undetermined (can possibly calculate from WPs but wound up using the empirical model anyhow). We also passed the beam thruogh a few optics and a vacuum window in order to actually hit the atoms, and the effect of the optical birefringence, angle-dependent polarization shifts from reflective mirrors, et cetera, would mess with this. To estimate the polarization we set up a Rochon prism after the beam exited the vacuum chamber through the LVIS hole and

calculated the circularity of the light. We compared with measurements taken at the centre of the beam axis before the window and found they were - how different? - this introduces an error margin of the light polarization of, well, some amount, and this manifests as a variable systematic error in some silly way.

Unfortunately we did not have the ability to measure the pointing of the magnetic field in the trap. This meant we were unable to find the precise angle between the probe beam wave vector and the quantization axis - hence the precise polarization in the atomic frame was not possible to determine as a function of measured parameters before the experiment. We constrained the direction of pointing to within 4 degrees (in polar and azimuthal angles)? Or we estimate that it was BLAH degrees based on simulations of the magnetic trap (estimate systematic error here). Fortunately, somehow this is absorbed into the fit so it doesn't matter in the end. Will need to revise this procedure.

What goes in here?

Hyperpolz?

Next? Isotope shifts? Precision required?

Key findings

Section wrap

Link to next part

Inflection point

Part III

Many-body physics

The nature of things

Collective phenomena

Quantum at scale

It to bit

Over the horizon

"From the Tao comes one, from one comes two, from two comes three, and from three comes all things." - Lao Tzu

Section introduction
Statistical physics Phase transitions
Thermal, quantum, dynamical, computable, semantic Emergent complexity

The third section of this thesis transitions from the study of atomic structure to the emergent dynamics of interacting systems. In teh old essay 'More is different', there is an argument that when you put a lot of thigns together they start acting in genuinely novel ways. A single water molecule is not wet - nor does it mean anything to say it is any given phase, or that is has a temperature. (this is of course problematic because it ascribes a specific state but the idea's there I guess). So ya. One of the watershed(?) moments in the history of physics was the *derivation* of thermodynamics from statistical mechancics - the assumption of a set of postulates about the microscopic nature of the world that led through the law of large numbers to a new understanding of empirical laws of the past; this gave a framework to understand and extend thermo, and it was a triumph to provide systematic ways to determine macro physics from teh nature of interactions. What was more profouond was the discovery of universality classes - that at phase boundaries there were unifying properties across disparate systems, things that tied together quite general phenomena in terms of these scaling relationships. This is kind of garbled. But yeah, look, we have agaaghagha this is just insane rambling - I wonder if I can push to 10k words in the process of smooshing out all this. Not an entirely honest drive if I'm honest but w/e the thing is I'm here and I'm writing even if it's completely useless and will get trashed. This is a start, even if it's bogus and hard. Anyhow back to progress. So ya - statistical mechnics also provided an actual understanding of temperature as a sublime phenomenon in all the emergent phenomenon - that really, at the end of the day, thermal equlibrium and the 'spontaneous' processes we see in nature are just outcomes of, basically, the law of large numbers. Phase transitions have been noted in all kinds of places now; the BEC transitiion is a classical phase transition. The idea is that an *order parameter* changes value from zero - representing a kind of disorganization - to something nonzero, representing an emergent order. These come in different flavours and in different systems but tied together by their scaling laws

- universality classes. Something really beautifully profound there. And of course, pepole have tried to take the numinous idea of the phase transition, of the *qualitative* change in the emergent properties of otherwise unchanged constituents, just by fiddling how they relate to each other - and staple it to all kinds of things. People talk of phase transitions in general network theory, presumably in social dynamics, and more recently even in the study of grammars, arguing that meaningful language corresponds to a marked phase transition in lexical trees. But turning back from flights of fancy - thermodynamics unified these ideas (in the earlier days) with the idea of *Free energy* which has since run rampant. But the idea is that - well, if you have tunable parameters, then are there different solutions to some equation? How do you wind up with these multiple free-energy landscapes from a microscopic basis? Or do you need to staple models toether? Idk, this would have been a great topics for a PhD, hey?

Regardless. The idea is that we should probably add more signposts to this meandering mess. I want to lead from classical phase transitions to order parameters - using BEC as an example, identify its universality class, no need to list off a ton or ramble about them too much. Then say hey, once you're in the ground state, you have different kinds of phase transitions. Quantum phase transitions, which aren't driven thermally or by statistical laws but by the structure of the gruond state, and they were first observed in an optical lattice. Free energy comes up as should correlations, I think, as they both come hand in hand with order etc.

Chapter 5

Quantum depletion of a harmonically trapped Bose gas

Chapter to-do

Make a real nice picture of a BEC...

- Intro/Theory
  - Spend 2x half day with correlation calcs predicting shape/amplitude
  - Depletion theory - scaling wrt N, n...
  - Thermal occupation of Bogoliubov modes; Temperature dependence of contact?
- Methods
  - Sequence diagram
  - Dark count rate determination
  - Can we obtain single-bundle temperatures?
  - Trap freq from number??? Temperature calibration?
  - Trap switch-off curve?
  - Verify method with Metropolis-Hastings and bootstrap
  - What if you relax the alpha=-4 constraint?

5.1 Introduction

Interactions between particles are a fact of life that theory must confront in attempts to phenomena. Modern experimental techniques allow access to a large range of interaction strengths, sometimes within otherwise identical systems. For example, optical lattices or Feshbach resonances can be used to tune interaction parameters

between extreme values, from the so-called strongly correlated regime (of great interest in itself) to extremely weak or even interaction-free (?) regimes. A common element in many of these experiments is the use of Bose-Einstein condensates (BECs) or degenerate Fermi gases as test systems for theoretical descriptions of interacting gases. What is quantum depletion? Why is quantum depletion interesting? What is the state of current knowledge? What does this paper contribute? How did we make our measurements? How do we interpret the results in context of current research? What else should we measure to further understand?

5.2 Physics of the condensed state

5.2.1 Properties of degenerate bose gases

The criterion for condensation is, roughly speaking, when most of the particles in a dilute bosonic gas occupy the same quantum state. More formally this is captured by the Penrose-Onsager criterion, wherein a homogeneous gas is said to be condensed if there is a macroscopic population of the ground-state eigenvalue of the ensemble density matrix. Any particles not in the ground state are said to be part of the depleted fraction. The depletion of the condensate is comprised of two parts, the thermal depletion and the quantum depletion. The thermal depletion is an artefact of the finite temperature of the condensate and has a number distribution described by Bose-Einstein statistics. The quantum depletion is a consequence of particle interactions/quantum fluctuations?

5.2.2 Bogoliubov theory and superfluidity

Bose einstein condensates are like really cool. BEC was predictedby Bose then translated by Einstein but there's some historical controversy here. BEC is a coherent state and connected intimately to superfluidity - the superfluid part of a SF BEC is predicted by lookig at BE statistics and taking the temp to zero. This means that you get lots of bosons in the ground state - wow, loo kat that, they're all doing the same thing! BEC is actually a measure of disorder versus distinguishability maybe? Like you could condense at a higher temperature if the gap is really big. BEC in a harmonic trap: Critical temperature, condensate fraction, chemical potential, peak density, thomas-fermi radius, momentum distribution, thermal fraction. BEC physics: Nonlinear Schrodinger equation approximated by GPE in the mean-field approximation BEC is actually, in practise, dependent on interactions between atoms. They need to thermalize as you cool the sample with evaporative cooling, although there are some folks who claim steady-state BEC by optical cooling which doens' t need th atoms to talk to ech other. But anyway, the meanfiled part of the condensate hamiltonian means your single particle states arent eigenstates ## Context & Gap Bogoliubov theory & superfluidity Connecting contact, momentum distributions, and correlations. French disagreement Contact measurements Probably about time to

write a review paper on experiments, no? ## Aim & scope
To reproduce the Palaiseau experiment. Applicability of Bogoliubov theory in optical lattices https://www.nature.com/articles/nphys1476 ¡https://www.nature.com/articles/nphys1476¿ The Bogoliubov approximation is justified whenever na_s^3 is small, i.e. low density or weak scattering, when the depleted fraction is small. In this case, in three dimensions, the depleted fraction is $8(na_s^3)^{1/2}/3\pi^{1/2}$ in terms of the s-wave scattering length, or $n\xi^d >> 1$, with the healing length$\xi = \hbar/\sqrt{2mgn_c}$ and $g = 4\pi\hbar^2 a_s/m$.

5.2.3 Quantum depletion in degenerate gases

A recent experiment [**Chang16**] observed quantum depletion in the large k tails of an interacting BEC released from an optical dipole trap, using the high-resolution and large dynamic range of detection offered by ultracold metastable helium atoms (He*) [**Vassen2012**]. A separate experiment on a strongly interacting BEC in a uniform potential probed with Bragg scattering showed that the depletion could be tuned with the interaction strength [**Lopes2017**]. However, current theoretical understanding [**Qu2016**] is that the depletion should not be observable after trap switch off in the presence of interactions.

During the expansion, which is taken to be hydrodynamic, the contact parameter tends to zero, which eliminates the depletion tail for sufficiently long expansions. This viewpoint was supported by an earlier experimental result that failed to observe the tails [**Makotyn2014**]. However, it is unclear whether the high momentum tails, which are by definition fast moving, are in fact accurately described by this model or if their shorter interaction time with the high density region of the BEC (in a semi-classical picture) means they do in fact survive the expansion.

To attempt to resolve this problem, we follow a similar method to [**Chang16**], where we observe quantum depletion of a Bose-Einstein condensate released from a magnetic trap, evident as a long tail at large momenta with the density scaling as k^{-4}. The values of the Tan contact constant we measure are slightly larger than those predicted by Bogoliubov theory in the local density approximation, although the discrepancy is smaller than for the results reported in [**Chang16**]. Our observation suggests that the results seen here and in [**Chang16**] are not an experimental anomaly, but rather demand deeper theoretical investigation to determine why the tails survive the trap switch-off and subsequent expansion.

A Bose-Einstein condensate (BEC) forms when a system of bosons is cooled below a critical temperature, where the majority of atoms occupy the ground state of the system. At non-zero temperature, the condensate will be depleted by thermal excitations, where some atoms occupy higher energy states with occupation probabilities following a Bose-Einstein statistics. However, even at absolute zero, the condensate will still be depleted by quantum fluctuations, a phenomenon known as quantum depletion.

Bogoliubov transformation

The BG transformation is of the form

$$a^\dagger(\mathbf{k}) = u(\mathbf{k})b_\mathbf{k} + v^*(\mathbf{k})b^\dagger_\mathbf{k} \tag{5.1}$$

I think. Then the number operator goes like

$$\langle n(k)\rangle = \langle a^d agger(k)a(k)\rangle \tag{5.2}$$

$$= \langle |u|^2 b^\dagger_\mathbf{k} b_\mathbf{k} + |v|^2 b_\mathbf{k} b^\dagger_\mathbf{k} + \text{cross-terms} \tag{5.3}$$

So the first term $\langle b^\dagger b\rangle \tilde{e}^{-\beta E_n} * dos$, by Bose-Einstein statistics - this is the thermal depletion. The last term is the quantum depletion. Where do the cross-terms go? What is the thermal population at high k?

This shows the interaction-induced quasiparticle vacuum has some effect on the single-particle states, modifying their momentum distribution.

Read Tan to figure out where the 4 comes from

The spectrum of fluctuations in the quasiparticle vacuum gives rise to an asymptotic momentum distribution that follows a k^{-4} power law[**Qu2016**].

The quantum depletion is a finite non-condensed fraction at zero temperature, arising from quantum fluctuations around the mean-field approximation to the condensate. The deformation of the condensate by the mean-field term in the GP equation does not lead to depletion. The authors comment that the depleted fraction may be *less*, and not *more* quantum than the condensate. Nonetheless: the depletion that follows is the quantum depletion as opposed to the thermal depletion: It is given by integrating the momentum fluctuations

$$\delta n = L^{-d} \sum_\mathbf{k} \delta n_\mathbf{k}$$

The far-field density of a harmonically trapped condensate is described by contributions from the condensed, thermal, and depleted populations,

$$n(\mathbf{k}) = nBEC(\mathbf{k}) + nT(\mathbf{k}). \tag{5.4}$$

The momentum density of the thermal fraction is [Pitaevskii & Stringari]

$$nT\mathbf{k} = \frac{1}{(\lambda T m\bar{\omega})^3} \tag{5.5}$$

$$g^{3/2}\left(e^{-\beta k^2/2m\hbar^2}\right) \tag{5.6}$$

where $T$is the temperature,$\lambda T = h^2/\sqrt{2\pi mkBT}$is the thermal de Broglie wavelength,$\bar{\omega}$is the geometric mean of the trapping frequencies,$\beta = 1/kBT$is the thermodynamic Beta, and$g3/2(z)$is the Bose integral

$$g^{3/2}(z) = \frac{2}{\sqrt{\pi}} \int 0^\infty \frac{\sqrt{x}}{z^{-1}e^x - 1} = \sum l = 1^\infty \frac{z^l}{3/2}. \tag{5.7}$$

The short-wavelength density of the BEC momentum density is described by the Thomas-Fermi approximation. The asymptotic momentum distribution is that of the quantum depletion,

$$n(\mathbf{k}) = \frac{C\infty}{(2\pi)^3 k^4}, \tag{5.8}$$

where$C\infty$is the universal Tan constant, defined by$\mathcal{C}\infty = \lim\mathbf{k} \to \infty(2\pi)^3\mathbf{k}^4 n(\mathbf{k})$, and for a harmonically trapped Bose gas is $\frac{64\pi^2}{7} as^2 N0n0$ in the local density approximation Chang et al The asymptotic behaviour of the single-particle probability density function for a particle in the ground state (not in the thermal fraction) is therefore$\frac{64\pi^2}{7} as^2 n0$, hence the contact constant can be seen as a parameter defining a probability distribution, which we estimate using the procedure described in the next section.

5.3 Methods

This section is divided into two: First, the details of the experimental setup used to obtain the data and a description of the relevant technical stuff. The hardware, if you will. In this section I first enumerate the types of shots taken and the entire sequence design, and then in the second subsection I describe the details of each of the calibration and measurement sequences in turn.

The second subsection concerns what happens after the data has been collected, as in how the data was processed in MATLAB software to obtain the Tan contact constant from the TXY data acquired from the MCP-DLD detector stack.

Processing My general dream for these sections is a graph of the program or some kind of systems diagram, maybe nested screenshots or pseudocode would do the trick and then include the code as an appendix hey?

After release from the trap the atoms expand ballistically into the far-field regime, where their position on the detector corresponds to their momentum after trap release by $\mathbf{k} = m\mathbf{r}/\hbar t_{tof}$, where t_{tof} is the fall time to the detector. Therefore we can reconstruct the far-field momentum distribution $n^*(\mathbf{k})$ from our detector data. The observed momentum profile $n^*(\mathbf{k})$ cannot be identified completely with the in-trap momentum distribution $n_0(\mathbf{k})$ as repulsive interatomic forces distort the profile immediately after release from the trap. redIs this basically the argument for why we see the increased depletion?

- Our bespoke software interfaces with the LabView control environmentand loops over a sequence of experiments, consisting in this case of: Atom number calibration, Trap frequency calibration, and RF transfer efficiency, followed by 10 data collection runs. - To calibrate the atom number, we used an RF pulse sequence to create a pulsed atom laser with intensity well below the saturation threshold of our delay-line detector. We corrected the number of detected atoms to account for the quantum efficiency (∼8 -) of our detector. - blueShould use QD measurements to compute condensate/thermal fraction relative sizes and further improve N_0 measurement. -

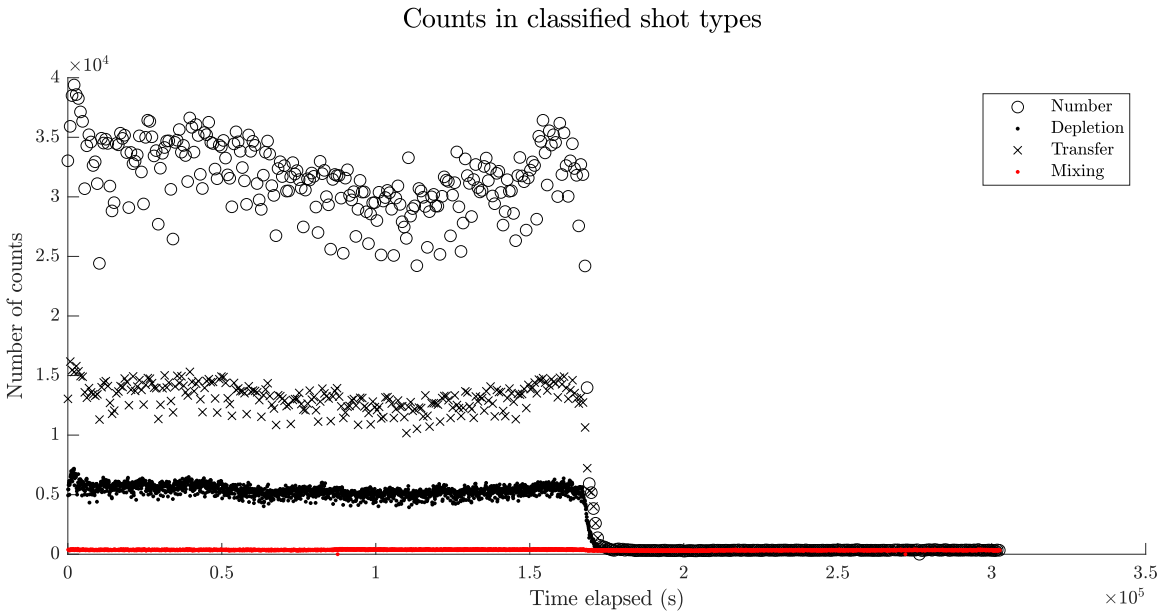

Figure 5.1:

bluehow does this compare to our trap binning? What is the uncertainty of the QE? - Together with the atom number, a measurement of the centre-of-mass motional frequencies allowed us to compute the peak density of the condensate. We measured the trap frequency by transient magnetic fieldto the trapped condensate for $\sim 150\mu s$, forcing centre-of-mass motion in the lab frame. We used the same pulsed outcoupling scheme as in the number measurement, and measured the centre-of-mass momentum of the cloud at the time of each pulse. Our outcoupling frequency is well below the natural frequency of the confining potential so we used a subsampled reconstruction method to recover the trap frequency. Prior to running experiments we varied the outcoupling pulse frequency to determine in which Nyquist zone the actual trap frequency lies relative to our sampling frequency. We can then obtain the trap frequency to within precision X in a single shot of the experiment by taking a Fourier transform of the centre of mass motion. - Our calibration sequence provided accurate number and peak density measurements along with the condensate profile. We verified the spherical symmetry of the thermal and depleted fractions, and so compute the momentum density by an average over a large section of the momentum distribution.

5.3.1 Data collection protocol/timestamping classification etc

5.3.2 Detection of ultradilute momentum spectra

Our experiments start with a condensate of helium atoms in the $m_J = +1$ state of the metastable 2^3S_1 manifold in a BiQUIC magnetic trap [**Dall2007**]. The strongest

signal of the depleted tails could be obtained by releasing the BEC from the trap and examining the tails of the detected flux on the detector. However, the presence of stray DC and transient fields in the chamber would distort the BEC profile and thus also the depletion, in ways that may not be feasible to characterize. For instance, it is known that our freefall zone contains what is colloquially known as a 'magnetic aperture', which deflects atoms from their freefall trajectory if their transverse momentum is great enough. This effect is visible in NONEXISTANT FIGURE, which shows the distortion of a thermal cloud, which would otherwise be isotropic. Indeed, this feature proved problematic in determining the detected count rate from the depleted fraction, because . Following the method described by Chang *et al* [**Chang16**], substantial distortions to the condensate can be avoided by transferring part of the sample to the $m_J = 0$ state, which is insensitive to stray magnetic fields.

Since for these experiments a precise knowledge of the total atom number and trap frequency is important, we measure the trapped population and trapping frequency at regular intervals throughout each experimental run, using a procedure that avoids detector saturation to measure the atom number and precise determination of the trap frequency. We identified a contamination of the depletion signal by stray counts attributable to the m=+1 state, and calibrate for this by including shots without the RF transfer step. We also apply corrections for the detector dark count rate and an increased background rate on the leading edge of the condensate, which is attributed to a steady-state leakage of atoms from the trap, due to Majorana flips, Penning ionization, or other collisional effects driving loss.

A magnetic field gradient is switched on 5ms after the state transfer pulse, which ensures the magnetically sensitive $M_J = \pm 1$ states are deflected enough to miss the detector.

Since for these experiments a precise knowledge of the total atom number and trap frequency is important, we developed an experimental procedure to regularly calibrate the trapped population and trapping frequency at regular intervals throughout each experimental run, using a procedure that avoids detector saturation to measure the atom number (see supplementary material). We varied total atom number between 1 and 5×10^5 atoms per condensate by varying the endpoint of the evaporative cooling ramp.

We use two trap configurations with characteristic frequencies $\sim 2\pi \cdot (312, 312, 52)$ and $2\pi \cdot 666, 666, 69)$ Hz, which were calibrated on setup by the pulsed atom laser method described earlier in chapter XXX.

As in previous chapters, data acquisition shots are interleaved with calibration measurements to predict the key variables

The trap is switched off in $\sim 100\mu s$ and the atoms allowed to fall 848mm, where they are detected with a multi-channel plate and delay line detector [**Manning2010**]. To avoid distortion of the condensate by stray magnetic fields, we transferred approximately 25 - of the condensate into the magnetically insensitive $M_J = 0$ state by applying a chirped sine wave 2ms after trap switch-off, swept from 1.6 to 2.6 MHz in 1ms, while a DC magnetic field remained on to preserve the Zeeman splitting between

$M_J = 0, \pm 1$ states. A magnetic field gradient is switched on after the state transfer pulse, which ensures the magnetically sensitive $M_J = \pm 1$ states are deflected enough to miss the detector.

After release from the trap the atoms expand ballistically into the far-field regime, where their position on the detector corresponds to their momentum at trap release. Therefore we can reconstruct the far-field momentum distribution $n^*(\mathbf{k})$ from our detector data. The observed momentum profile $n^*(\mathbf{k})$ cannot be identified completely with the in-trap momentum distribution $n_0(\mathbf{k})$ as repulsive interatomic forces distort the profile immediately after release from the trap. Structure is visible over five orders of magnitude in density, comprised of the condensed, thermal, and depleted fraction before the signal drops below the dark-count background noise. There is some saturation evident around the low momentum values due to the high atom flux during BEC impact. Our analysis does not include this part of the momentum profile, and we find evidence that saturation is only an issue during the peak flux, not in the thermal or depleted fractions.

The count density from the falling BECs depend explicitly on the trapped population and on the trapping frequencies, necessitating regular calibration of the peak condensate density. The correction from the detected $m_J = 0$ counts to the full condensate profile also requires a measurement of the transfer efficiency of the RF pulse, and a diagnostic of any other sources of detection events, such as detector dark count rate or remnant atoms from the $mJ = \pm 1$ condensates. In the remainder of this section, I describe the means by which the relevant parameters are calibrated and how they are combined into a model of the detector flux which includes the Tan contact as a free parameter. In the next section, I describe the algorithm I designed to transform the atomic detection events into an appropriate format to correspond with the model and determine the Tan contact.

Contributions to the model

Depletion

In an ideal world, the experimental procedure is trivial: Form a BEC in a desired trapping configuration, and then release the trap instantaneously and fit the atomic density profile obtained from the DLD image. Unfortunately, nature intervenes: Because our condensates are formed in a weak-field-seeking state, they are subject to deflection during freefall by stray DC and transient magnetic fields. These distortions to the BEC profile may be significant at large momenta, although we did not characterize this. A second potential issue is detector saturation, whereby the trailing side of the BEC is detected with a lower quantum efficiency because of a depletion of charge carriers in the MCP, artificially attenuating the depletion signal. Both of these issues are ameliorated by transferring a fraction of the condensate into the magnetically insensitive $m_J = 0$ shortly after the trap release. This is achieved by sweeping an RF pulse from 1.6MHz to 2.6MHz, as in [**Chang16**], with a DC bias field held on by the Nuller coils. This field is close to uniform over the scale of the BEC and its freefall

path, so by the time the condensate is split into the three spin states, distortions to the cloud would be minimal.

The detection sequence therefore proceeeds with a standard BEC production sequence (as described in INTRODUCTION), with a modified end sequence, pictures in figure QD-SEQUENCE. The DC bias field is ramped on over 300ms in an exponential ramp with time constant 40ms. This ensures that no centre-of-mass oscillations are induced in the BEC because of sudden displacements of the trap centre. The BEC is held for XXX ms to damp out any residual oscillations and is then released. After 2ms of freefall, the RF chirp is generated by a RIGOL function generator, amplified, and applied to the experiment chamber by a coiled antenna inserted into the BiQUIC coil housing. The nuller coils are switched off, and the auxiliary push coils in the vertical (Z) and weak horizontal (X?) axis are activated via fast MOSFET switch. The pulse timing and duration of the push coils required some finessing to minimize the scatter of atoms from a *magnetic aperture* inside the freefall path, as described in later in this section. The push coils remove the $m_J = \pm 1$ atoms from the detector, so the detector signal is dominated by the undistorted $m_J = 0$ cloud. The cloud then falls freely under gravity through the vacuum chamber, completing the 848mm fall in 417ms.

It is important to align the condensates carefully in order to faithfully extract the large-momentum tails. With an ideal detector, one could simply take the mean of all detected counts. Because of detector saturation, however, the mean position is heavily biased toward the leading edge of the BEC, and indeed the median (which is robust to outliers) is biased also (it is less robust to skewness). A workaround can be found in the threefold reflection symmetry of the condensate: The parabolic profile in each principal axis means that if one can identify the edges of the condensate, the centre of mass is at the midpoint along each axis. This is the basis of the following centering algorithm: For each axis, the atomic detection events are compiled into a histogram as a discrete approximation to the continuous atomic flux. The region where atomic flux exceeds the background rate by a factor of X is determined to be the BEC region - the extremal positions (or times) with flux above the threshold determine the edges of the condensate, and the mean of these two values determines the centre. The stages of this algorithm are depicted in figure CENTERING, along with the variation of the BEC centre over the course of a run.

We are concerned with the momentum-space distribution of counts. The atomic wavevector is related to the in-trap velocity by $\mathbf{p} = \hbar\mathbf{k} = m\mathbf{v}$. The tranformation from $\mathbf{r} - \mathbf{r}_0$, where $\mathbf{r}_0$ is the centre-of-mass position, is simply a linear transformation $\mathbf{v} = \frac{\mathbf{r}-\mathbf{r}_0}{t_{tof}}$ in the x and y directions. For z, corrections must be made for gravitational acceleration instead given by solving the ballistic trajectories $v_z = -h/t_{tof} - \frac{1}{2}g * t_{tof}$ where h is the fall distance and g is the acceleration under gravity. txy-to-vel vs linear error?

The centred velocity-space counts are then transformed into spherical polar coordinates. The algorithm is described here is also used for the spin-mixing and dark

count calibrations, where the spherical coordinate system is centred at the mean BEC centre-of-mass position in TXY coordinates.

$$(r_i, \theta_i, \phi_i) = (\sqrt{x_i^2 + y_i^2 + z_i^2}, \tan^{-1}(y_i/x_i), \tan^{-1}(z_i/\sqrt{x_i^2 + y_i^2}) \tag{5.9}$$

The counts for each BEC are then compiled into a spherical histogram

$$N(R(n), \Theta(l), \Phi(m)) = |\{(r_i, \theta_i, \phi_i : r(n) \geq r_i < r(n{+}1), \theta(l) \geq \theta_i < \theta(l{+}1), \phi(m) \geq \phi_i < \phi(m{+}1)\} \tag{5.10}$$

Where n, l, m are indices of the histogram with edges $r(n)$. Ergh, get this notation sorted out. The memory demands can get exhaustive - holding large TXY datasets and also lots of large 3D histograms - can reduce the by lots of writing to disk, but the cheater way around this was to compute the mean by adding to the histogram by looping over each shot, and ditto the squared number of counts to find the variance later. There would also be a biasing effect by including the empty bins which are defined outside the detector area. These are found by a messy case analysis in `find_final_bin_idx.m` (hyperlink to dox html?). These are excluded from subsequent sums over profiles. The bins are normalized by the spherical volume element

$$V(n, l, m) = \int_{R(n)}^{R(n+1)} dr \int_{\Theta(l)}^{\Theta(l+1)} d\theta \int_{\Phi(m)}^{\Phi(m+1)} d\phi r^2 \sin(\phi) \tag{5.11}$$

$$= (\Theta(l+1) - \Theta(l))(Cos(\Phi(n) + \frac{pi}{2}) - Cos(\Phi(n+1) + \frac{pi}{2}))(\frac{r(n+1)^3 - r(n+1)^3}{3}) \tag{5.12}$$

CHECK THIS 3.

Flux model

The pointwise density of atom detection events in momentum space can be described by the expression

$$n(\mathbf{k}) = \sum_{m=-1}^{1} n_m(N, \omega_{x,y,z}, T, \mathbf{k}) + \delta(\mathbf{k}) + \lambda(N, \bar{\omega}, \mathbf{k})\Theta(-\theta) \tag{5.13}$$

The first terms n_m refer to the detected density of atoms from the $m_J = m$ condensates, which depends on the momentum vector on the total atom number N, the temperature T , and harmonic trapping frequencies $\omega_{x,y,z}$. The dark count rate δ is momentum-dependent due to its non-uniformity on the detector. While the BEC is held in the magnetic trap, it is subject to loss mechanisms such as Majorana transitions, Penning ionization, or three-body recombination, and so 'leaks' at a rate rate λ, which may also manifest a momentum-dependence because of its spatial non-uniformity on the face of the detector. When the trapped gas is released, the leak stops, hence the Heaviside theta function $\Theta(-\theta)$ ensures this term only contributes

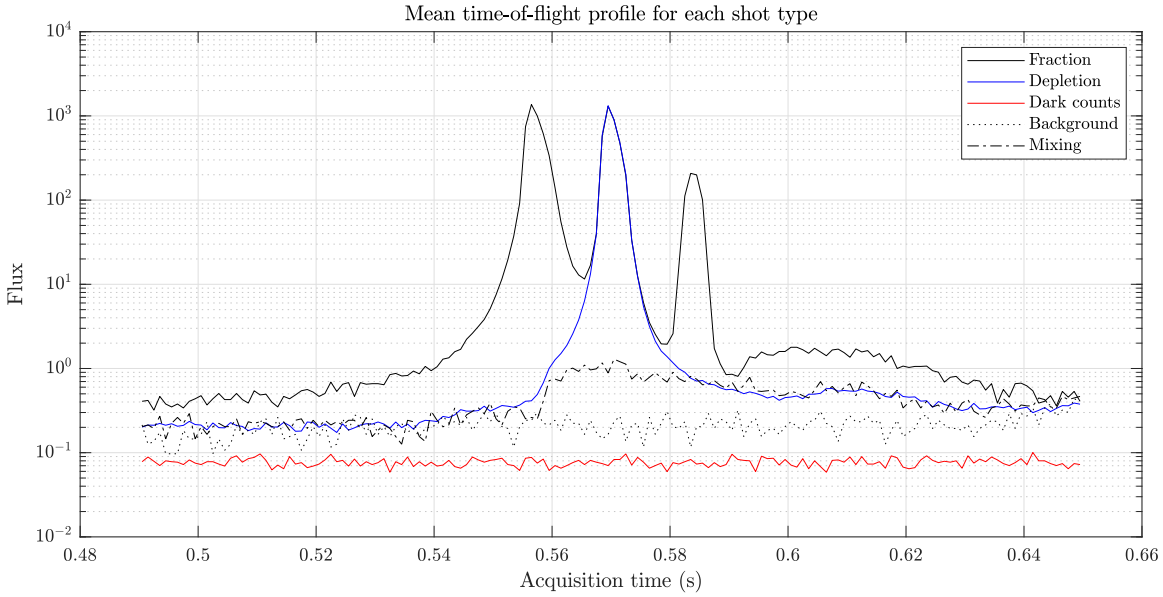

on the lower side of the falling BEC. The distortion-free depletion signal is found in the contribution $n_0(\mathbf{k}, N, \omega_{x,y,z}, T)$. The calibration protocol described in this section is designed to extract this by subtracting away the various sources of background counts, and also ensure accurate calibration of the experimental parameters N, T, and $\omega_{x,y,z}$

Peak density

The peak density of the condensate can be derived from the expression for the chemical potential $\mu = g\rho(0)$: (see [**PitaevskiiStringariBook16**], pp.181)

$$\rho_0 = \frac{\mu}{U} \tag{5.14}$$

$$= \frac{\hbar\bar{\omega}}{2}\left(\frac{15N_0a_0}{\bar{a}}\right)^{2/5}/4\pi\hbar^2a_0/m \tag{5.15}$$

Where N_0 is the total condensed number, $\bar{\omega} = (\omega_x \cdot \omega_y \cdot \omega_z)^{1/3}$ is the geometric trap frequency, $a_0 = 7.512$ nm is the interatomic scattering length [**Moal06**], m is the atomic mass, and $\bar{a} = \sqrt{\frac{\hbar}{m\bar{\omega}}}$ is the harmonic oscillator length . Thus the peak density of the condensate can be determined by a measurement of the trapping frequencies and the total condensate number. Fortunately, these parameters can be measured simultaneously with the pulsed atom laser method described in chapter TUNEOUT. As shown in chapter TUNEOUT, the trap frequency is stable to XXX accuracy. Therefore, even over runs of several hours, the trap frequency variation contributes only YYY much variation in peak density. The variation in atom number can be

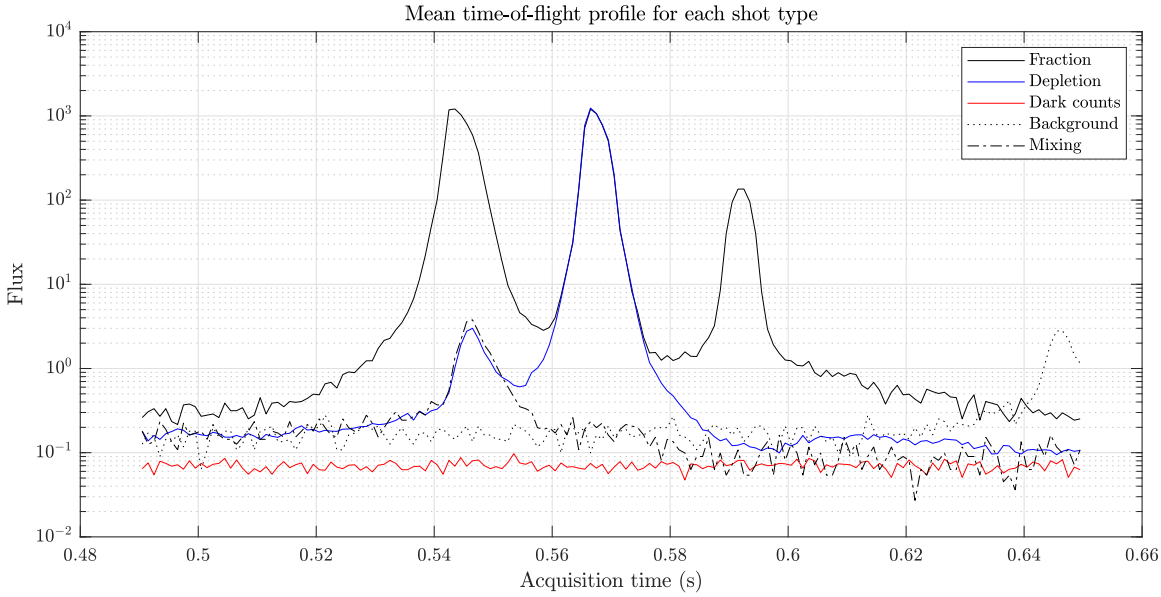

as much as XXX per cent, which corresponds to a YYY per cent variation in peak density.

Dark counts

Even when the Helium source is not active, the MCP-DLD detector stack stil registers detection events. These may be genuine, spontaneous electron detection events seeded by background gas in the chamber or thermal excitation in the MCP, or indeed by transients in the DLD lines that are sufficient to trigger a digital pulse from the discriminator. These are referred to as *dark counts*, by analogy to the Poissonian electronic noise in digital camera sensors like CMOS arrays. Indeed, the detector dark counts are uncorrelated events and so form a Poisson distribution Clarify & graph of dark count statistics. The correction for detector dark counts is entirely analogous to *darkfielding* in precision photography, where images are taken without a light source to correct for detector noise. The spatial distribution of dark counts is shown in figure FIGURE, the time profile in figure PROFILES, and the calibration procedure is described in the next section.

Dark counts Figure: Spatial structure and statistics

The dark count rate is assumed to be uniform in time. It may be altered by high atomic fluxes of the condensate itself, but this is not a concern for the following reasons: One, we observe very similar thermal tails both above and below the condensate, suggesting that, at least, the quantum efficiency and dark count rates are not significantly different. Two, although there are some temporary hotspots on the detector during the peak BEC flux, these are only observed co-temporally with the falling BEC. The quantum depletion is detected far beyond the regions where this effect is noticable, and so they are not expected to contaminate the signal.

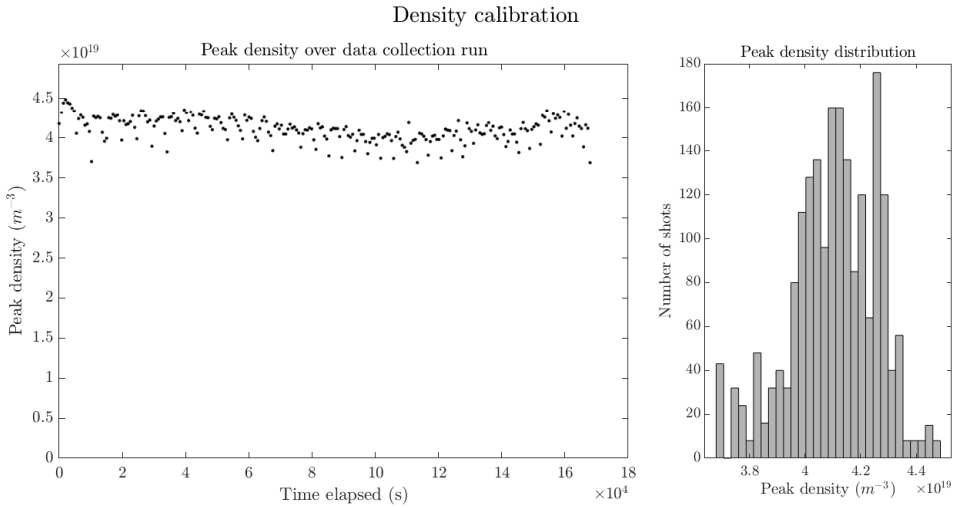

Figure 5.2:

A second source of background counts is the so-called *trap leakage*, which is a measurable increase in the steady-state count rate while a BEC is held in the trap, which is visible in figure **??**. Unlike the dark counts, the trap leakage has no obvious spatial structure. Correcting for these counts is therefore a matter of computing an average spurious count rate and then subtracting this from the detected count density, as described in the next section. Because the trap leakage stops when the trap is released, this correction is applied only to the leading side of the condensate.

The best way to deal with it would be to extend the hold for ages, and then get heaps of statistics, but in the end I wound up using the 20-odd ms window of hold before drop in each case. This still gets to within ??? some margin of error when using all the data I have for a given run. In reality, the leak rate should depend on the BEC number, as, for instance, Majorana losses would induce an exponential decay of the trapped atom number, and Penning ionization losses scale with the squared density. There would also be density-dependent collision effects feeding the trap leak rate driven by changing the trapping frequencies, and different trap configurations would change the trap centre position, which could affect the detected density of the trap leakage. However, the count rates are so low that we do have the sensitivity to these effects, and so take a relatively simplistic treatment of the trap leakage, described in the next section.

Transfer efficiency

The efficiency η_0 of the population transfer to the $m_J = 0$ state is critical in determining the Tan contact, as the factor $1/\eta_0$ is the correction applied to the final signal in order to estimate the true signal density in the original condensate.

The RF chirp transfers atoms into the $m_J = m$ states with efficiencies η_m. The chirp was adopted because, as described in [**Chang16**], it would minimize the momentum-dependence of the spin transfer pulse. The transfer efficiency cannot be calculated by counting the detected number in each cloud, as the condensates still saturate, leading to incorrect estimates. This is illustrated in figure SATCH-FRACTION.

Instead, we can take advantage of the fact that the condensates have identical spatial profiles (to within a good approximation), albeit with different amplitudes, c.f. hydrodynamic expansion - density-dependent effects v small after 2ms?

The momentum distribution of the thermal fraction of a degenerate Bose gas is known to be isotropic (see [**PitaevskiiStringariBook16**] pp. 160) and constitutes less than 5% of the total population throughout this experiment. The momentum distribution of the thermal fraction takes the form

$$n_T(\mathbf{k}) = \frac{1}{\lambda_T m\bar{\omega}} g_{3/2}\left(e^{-\beta(\hbar)k^2/2m}\right), \tag{5.16}$$

which is manifestly invariant under rotations about the centre of momentum. Therefore, integrating over the k_x and k_y directions resolves the k_z-dependence of the momentum distribution. (You can talk through the physics better than this matey). After centering the clouds using a thresholding procedure described in the **Depletion** section, the time-of-flight profile of each cloud is divided pointwise by the sum of all the time-of-flight profiles. In the regions where the detector is unsaturated, the ratios $n_m(\mathbf{k})/n(\mathbf{k})$, where $n_m(\mathbf{k})$ and $n(\mathbf{k})$ are the momentum-space density of the $m_J = m$ clouds and the original BEC, respectively, are estimates of the transfer efficiency η_m, as shown in figure . This figure also shows that detector saturation is not apparent in the thermal fraction of the trailing side of the BEC, and therefore suggests that saturation would be negligible in the depleted wings in the trailing edge. Further, the uniformity of the determined ratio across the thermal fraction is evidence that the RF transfer efficiency is independent of the particle momentum.

Compare Doppler width to RF pulse width; simulate ramp to guesstimate transfer efficiency, optimize ramp (autodiff?) to find maximum transfer rate).

Spin-mixing

In the depletion detection shots, we have observed a remaining presence of $mJ = 1$ atoms. These are visible in figure PROFILES, as the step-up in flux rate at 0.56s in a) and the peak in detector flux at 0.55s in b). The cause of which is unclear but is suspected to be due to a collision process with a feature inside the chamber, as illustrated in figure CLOUDSMASH. Regardless of the cause, we calibrate for this contamination (also called *spin mixing*). by running the depletion measurement without the RF transfer, instead measuring the time-of-flight profile of the $m_J = 1$ cloud. After subtracting the background rates as appropriate, this provides a suitable calibration image for the spurious counts, which is subtracted from the measurement profiles, weighted by the transfer efficiency η_1.

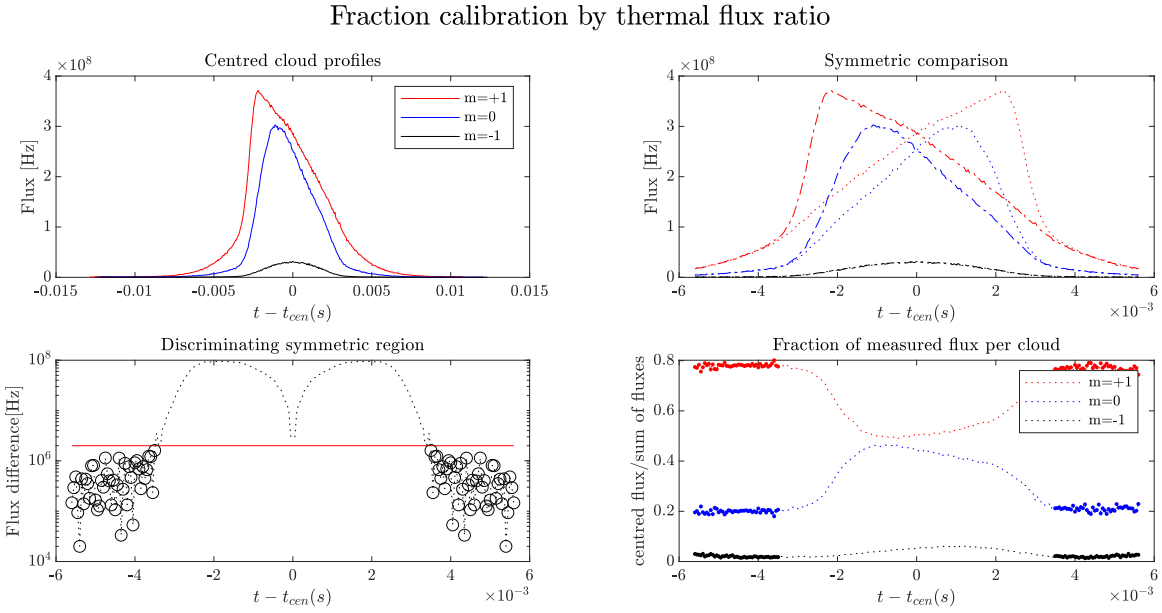

Figure 5.3:

The count density of the $mJ = 1$ states depends on the trapping frequencies, as shown by the clear difference between their contributions to figure PROFILES a) and b). This is likely because the trap centre and BEC width shifts with changing trap frequencies, so the push coil sequence would, left unchanged, result in different spray patterns on the detector. Unfortunately, we cannot rule out the presence of $mJ = -1$ counts on the detector without additional calibration (for example, taking yet another shot with a different RF transfer fraction). However, as the $m_J = -1$ clouds are determined to have about one tenth of the total atom population, and the $m_J = +1$ counts are suppressed by nearly three orders of magnitude by the push coils, if we assume a similar suppression of the $m_J = -1$ cloud then Worst-case bias of -1 counts

Allan variance of BEC centres?

5.4 Determination of the Tan constant

Fix terminology: TXY or KZXY data are *detection events* or *counts*. Histograms (or density data) are *images*

The fit to the depletion profile $n_0\tilde{(k)}$ is obtained by taking the weighted sum of the k-space images for the depletion, spin-mixing, and dark count rates:

$$\tilde{n}_0(k) \approx \frac{1}{\eta_0}\left(n_0(k) - \eta_1(n_1(k) - \delta(k)) - \delta_k - \lambda(k)\right) \tag{5.17}$$

To avoid detector hotspots and to ensure we only use angular bins which extend far enough in k-space to capture some depletion, we specify the spherical sample region $\{(r_k, \theta, \phi) : 1E6 < r_k < 3E7, \theta_{range}, \phi_{range}\}$. Averaging over the angular bins commutes with the image summation because they're all linear. This produces one-dimensional radial profiles, as shown in figure K-PROFILES. The depletion and the thermal tails are isotropic, but the BEC is not, so the BEC peak is not physically representative. Or, remove it from the plot so it's just thermal - i.e. plot from the largest TF momentum.

As in [**Chang16**] we find the large-**k** momentum distribution is isotropic, unlike the in-trap mean-field interactions, and conclude that the extreme momenta are not strongly affected by the mean-field. A typical condensate profile shown in Fig. **??**. Structure is visible over five orders of magnitude in density, comprised of the condensed, thermal, and depleted fraction before the signal drops below the dark-count background noise. There is some saturation evident around the low momentum values due to the high atom flux during BEC impact, however this part of the histogram is not used for the analysis.

The Tan contact parameter is extracted by a fit to BEC density profile after subtracting the calibrated noise profiles. The functional form

$$n_{fit}(k) = \frac{N_{th} g_{3/2} exp(-k^2 \lambda_{dB}^2/4\pi)}{1.202(2\pi/\lambda_{dB})^3} + \frac{C}{(2\pi)^3 k^4} + const,$$

includes contributions from the thermal fraction and depleted fraction and includes the free parameters N_{th} the number of thermal atoms, $\lambda_{dB} = h/\sqrt{2\pi m k_B T}$ the thermal de Brogliewavelength, *const* a constant to account for the detector background count rate, and C is the scale of the fitted power law assumed to correspond to the Tan contact parameter. In the local density approximation, $C \approx C_{LDA} = \int d\mathbf{r}[16\pi^2 \rho^2(\mathbf{r}, t) a^2]$, where a is the scattering length and ρ the atomic density. The initial guess for the fit constant C is set to Tan constant predicted by the peak density and number calibrations. The initial temperatures are set manually for each directory. The thermal and the depleted parts of the profile are fitted individually to better constrain fitting parameters, and then a joint function is fitted to find the best overall parametrization.

We verified the fitting method by analysing a test data set of known parameters, which was generated by the Metropolis-Hastings algorithm, and find the method recovers the test set parameters within a factor less than our experimental uncertainties.

5.4.1 Verifying the method

Verify fitting is faithful estimator; examine bias and stability for unconstrained powers
Reliably estimating the parameters of a power-law distribution is nontrivial[**Clauset09**], and the robustness of the fitting method above has not been exhaustively tested. The LDA prediction is essentially that the single-particle wavefunctions, hence the single-particle probability distribution over momentum, are affected by many-body effects.

One computes the single-particle probability density by dividing the condensate density by the number of particles (hence the N_0 term in the LDA), and then the problem of extracting the contact parameter from the data is an exercise in statistical parameter estimation. As shown by Clauset et al [**Clauset09**], fitting these functions tends to produce incorrect estimates of parameters. The method outlined in Clauset was proven to asymptotically converge with probability 1 to the correct fit parameters of a power law distribution, but would need to be extended to derive a maximum likelihood estimator for a power law overlaid on a constant background.

5.5 Discussion

5.5.1 Findings

According to theoretical predictions based on the local density approximation [**Chang16**], the contact constant C_{LDA} of the depleted fraction should vary linearly with the peak condensate density n_0. This was found in previous experiments[**Chang16**], although their scaling factor greater by a factor of ∼6.5. In Fig. XX, we plot our measured values of C and n_0 , identifying the fit parameter C with the contact constant C_{LDA} . A linear fit to the contact constant variation finds a gradient approximately 1.7 times more than the theory predicts.

Our findings suggests that the visibility of the quantum depletion in the far-field momentum distribution is indeed a real physical effect. Our findings are corroborated by theoretical work Simulation details. However, the question remains open as to why the observed population of the quantum depletion is greater than predicted by the otherwise successful Bogoliubov theory. Possible confounding factors:

- Intra-cloud scattering
- Trap switchoff or early-falltime dynamics,switch-off timescale may be relevant (compare [**Chang16**] with [**Qu16**]).
- $m_J = -1$ counts

We have assumed that the RF transfer is momentum-independent, but this could be violated by inhomogeneities or transients in the magnetic field. The RF pulse may increase the Penning ionization rate in the depolarized sample, even though the density is low, which would alter the momentum profile. While applying the magnetic separation pulse, the condensates may scatter off each other.

5.5.2 Future work

- Correlations would be the smoking gun
- Optimal transfer Time-varying 3LS hamiltonian?

A possible future experimental extension is to outcouple atoms using a broadened Raman transition. This would have the benefit of moving the outcoupled atoms through the cloud rapidly, minimising the effects of repulsive inter-atomic interactions that normally affect the outcoupled profiles. This should shed some light on whether interactions during trap switch off are the origin of the momentum tails. One could test the importance of particle scattering or Penning ionization by delaying the Rabi transfer to the $M_J = 0$ state, but this could increase vulnerability to stray magnetic fields. There is scope to optimize the RF transfer sequence to achieve much higher transfer efficiency for a stronger signal

Chapter 6

Towards an optical lattice for quantum simulation

6.1 Quantum ∩ Complexity

6.2 Optical lattices

6.3 A lattice for helium

6.3.1 Opportunity

6.3.2 Progress

6.3.3 Legacy

The previous chapter would have dealt with the case where interactions between atoms were present but weak, and so were amenable to solution by perturbative or approximate methods. This means taking a solution for non-interacting systems and making small corrections. The information about the microscopic behaviour can in some sense be averaged out, or accounted for in aggregate, producing a simpler picture that can be mathematically more tractable. There are many instances where the solvability of models is no longer guaranteed even approximately. These so-called strongly correlated systems are ones where the actual evolution is completely different from the non-interacting case.

Philosophica; digression: There is great power in mathematics, in teh ability to produce analytic results for a given model. That is, here is a set of assumptions about a description of the world, and so I can use this to do smoe efficient computation and predict the future state of the world, or some part of it. Models are paradigmatic in physics for this reason, and they represent a great deal of compression, of abstraction of patterns out of context. In some ways they - mathematical models - could be thought of as the quantitative storytelling part of humanity, the things that make it

unique - and so there's something really sublime about the exactness of the correspondence with the world, written extensively about in things like 'the unreasonable effectiveness of mathematics' and this correspondence is still explored in the problems of foundations of QM: what exactly does this mathematics say abotu the nature of the world? Why does it run this way? This deep inquiry will always be part of the human spirit, I think, but yeah. So, models are great. But you can only get them somtimes - if the algebra is nice, which is usually the case for simple, linear things, symmetric things, or where we can take the large-N limit as in the case of thermodynamics. But once things get more complex we may not have so-called closed form solutions. So we would need approximate methods. The modern incarnation of this is by algorithmic means - given boundary conditions we can solve DEs which are the foundational tool of physics. For probability distributions, rather than pointlike coordinates or vector evolution, things are more complex. That is, you need to worry about things like stochastic master equations and such which are very computationally expensive for quantum systems. There are analytic approximation methods too, using Feynman diagrams or computational tools inspired by them - but yeah that's way beyond scope here. Suffice to say they work - see LHC - but they're expensive I guess.

but the point I guess is that there is a wealth of methods that rely on the in-silico method: A digitized representation of the state of the system with some precision, and a method to evolve the state of the machine. THe problem is when you want to express a large - that is, many body and fairly strongly interacting - quantum system, and so the required memory is really big. That is, the state vector is exponentially large in the number of particles, and if you want to store the whole density matrix then things get much worse! And so we need other means. Approximations exist; consider only low-order correlations, for example, like the Gutzwiller methods, or find self-consistent solutions like in Hartree Fock. There are other methods of course - exact diagonalization is the best in the sense that it is, well, exact. And the scaling isn't *too* bad for matrix inversion, and once you're done you're done. The thing is you need the memory to store the matrix and thigns get bad pretty quick. And this is just for simulation of dynamics that evolve under a stationary hamiltionian. TImevarying stuff is probably a lot worse - quenches are OK to model and correspond to strongly diabatic changes in stuff, but ya. The upshot is that using existing machines to simulate stuff is OK, but really limited.

Why is this a problem? Well, large-scale systems are ones we'd like to understand. Superconductors for example. Or big proteins/drugs. Or photosynthesis. So what's the problem? Well, quantum is paradoxically complex; a state vector requires so much infomaiton to describe, but only gives us a sliver of that when we measure it. And nature doesn't seem to have any worries runnign these quantum systems itself. So why not just use these analogies? Use a quantum system to represent a quantum system? You're still faced with the input and output challenge - state preparation is expensive, readout is expensive - but for some processes you mgiht not need big superpositions or massive entangled states, which are much harder to produce (look at some of these scaling results hey), but output is always gonna be an issue I guess.

Unless you're really judicious with your output and manage to transform the states you care abotu into ones that are orthogonal in yuor measurement basis I guess. But that's another story. The idea is old; back to Feynman in, what, the 80s? So I guess it's not that old and took off really fast! Best to get a date on that one.

So the posterchild for this kind of solution is the general quantum computer - one who can initialize a many-body quantum system in the ground state, then apply arbitrary unitary operations to it. This could include simulating time evolution or by using the quantum state vector as a superposition of computing states, to run calculations. So this would be more like quantum logic. In the end it's all the same. But building an arbitrary hamiltonian is beyond us rn. Fortunately it turns out that all you need is to be able to generate a basis of the lie algebra of transformations that you could peform. And some smart buggers proved that for large quanutm states you can do it with a universal gate set - for universal digital quantum computing at least, which is capable of enacting any unitary operation, and so this includes time evolution of quantum systems. I wuold like to check the equivalen t for time evolution - trotterization isn't quite this, as it boils down to some fairly complicated stuff. There's a whole swath of computing architecture out there right now, and several compilers that will take an operation and break it down into the gate set, so you can just write out your inifinitesimal unitary and go for gold. But yeah, approximation errors. So i think this cahpter needs a lot more focus. And I would like to better understand the problem classes that are within simulation - it's not quite the same as the complexity classes, I guess, but i wonder if you could phrase them as SAT problems if you're trying to make predictions? Tough to generalize exactly what people look for.

Alternatively, well, quantum simulation. Thatis, analogue simulation. Thisidea is a bit less sophisticated than full quantum computing but turns out that there's a map the other way for example some lattice models ahve been shown to be universal, which means that for special choices of the coupling constants one can actualyl get full universal computation - simulating a digital quantum comptuer. Of course this is a completely other technical challenge, requires ptoentially long-range coupling, so your hardware gets really tricky especially for long-range entangling operations, et cetera. So yeah, not super easy. But in the case of specific problems, well, you might nnot do so badly. I wodner if you can scale problems from interacting graphs to equally-coupled models with on-site potential variations. Seems hard, as you'd rapidly increase the number of atoms yuo need, and probably some bizarre modulation on the lattce depth but something worth having a bit of a think about wen writing this chapter anyways. So yeah. Uhm. Im supposed to be writnig abotu quantum simulation; the analogy bbeing a wind tunnel, say, rather than building a digital sim. That said, now the task is usually done extensively in silico because it's *faster* and also because it's usually *cheaper* - human time is still expensive when you could use -perhaps more- energy in silico for suepr cheap thanks to the economies of scale. Of course, it's not clear when QCs will reach this kind of scaling,a s they need to be error-corrected which is not currently possible at any kind of practical sense, but it's

still something people will shoot for. And actually this underscores the issues or the advantage of runniing quantum simulation ebcause well, yeah, there is noise, but for some kinds of noise one hopes that the contribution is someqhat gaussian, right? So you're still gonna try to monte-carlo your way aruond, except you're sampling from physical analogs. The first example of this was Greiner & Bloch, good on 'em. the idea was pitched by Zoller. IDK why they didn't go straight for fermions, but thats' how it went. This would be a good thing to cehck out, the historical reasons. And the key papers therein I guess. but why? For the sake of a good read, and well, yeah, they're kind of the seminal papers in the field! So best go get 'em. Sho wat comes next? Um. I was on the tangetn about analog simulators, so there would be space for a survey of the field here. Starting without too much delving into specific models, but that would be a good look at the best in the world, or the first - various lattice geometries, magnetic lattices (how they doing?) And quantum gas microscopes - but then hey look ma, as we talked about in earlier chapters, they're not able to resolve single-bdoy momentum spectra. So this is why we would care about using BEC of He* - currently the best way to do this at scale. Some people have done few-fermion correlators recently (See the thermal correlator/dipolar fermion paper is it?) - but this would be really hard to scale, right? I wonder what the limitations are here. Or could you use a kind of torque to take longitudinal momentum into a lattice-free potential? LIke, use a different dimension of a 2D lattice for this. It's also worth talking about the state of the art of QMC - people have done 3D bose hubbard right, and done exceptionally well. DOes this sort of shoot the project in the foot? I wodner. Something to check out. BUt then yeah we get to talk a bit about the Bose HUbbard model.

[If I don't get to it in the previous chapter re: Bogoliubov and quasiparticles, thsi woul dbe a good plcae to dig into why we would care about momenum correlations.]. But then yea some extra goodies might be lifted/inspired by the french papers... 1-body momentum measurements in optical lattices metastable He: start with bosons Bose-hubbard model Consdier a 2-well example; look at the quantum phase transition. Then what. Well, how abotu the 2-body momentum spectrum for BH coupled wells, huh? That'd be a nice illustration. There's probably room to talk about these as arrys of josephson junctions - a good chance to try and understand those if you want to. BUt that'd be an optional part I guess. Part of the survey. Maybe worth tracking down some of hte theses from the Greiner & Bloch labs. ## Aim & scope
To build the dang lattice ## Contribution Maybe it's best to do this chronologically. * Cut my teeth on AO alignment and eventually building a MOT with an old-school security camera * Assembling new vacuum system Construction Bakeouts - logs? Ti Sub and NEG improvements * LVIS * MOT 2 * Absorption Imaging * Dipole alignment * Misadventures and eventual fluke - thanks to Patrick

Vacuum chamber

Optics build inc dipole So when I started, we actually didn't have a working MOT. THere were the optis but they were dirty and eyah. So they didn't have light either. Had to build a few AO arms - everything except the collimator and zeeman slower I

think, and the ZS was set up according to the old paper about that lab, right? THe 'optimized' one. Altough one could certainly design a chirped system to increase yield, but then I wonder what the density/number limits for a MOT are. How much could we actually obtain, given that we then have to push through the feed hold into another chamber? SO yeah. Two MOTs. Anythign exciting to write about? Maybe not - just ballpark the capture velocities maybe. The dipole diagram and control woudl be worth describing. The theory of dipole trapping would belong here as it's not really relevant? Oh, no, I'll have to put it in the alignment chapter - well it realyl sits in the polz part of the tuneout chapter. So that'll cover that I guess. Look over the simulations of the dipole potential. Maybe some simulations of evaporative cooling in the dipole. Open source 'em of course. Would be a fun way to try some auto-optimization algorithms for path optimization. Another way to burn some time, I guess, there are a lot of things in here that are becoming big to-do items! Bu Sequence up to evap & dipole Imaging system Diagram, some example images and calculation of number Small simulations ## Progress meanwhile
New coils, solder catastrophe, new plates ## Issues/What next Stability: Vibration, temp, vacuum Optics: Power, profile Automatic optimization Broad goals Fermions Quasirandom lattices Are these actually resources or what? Next generation laser tech?

Epilogue

Synthesis

Outlook

Afterword

Gratitude

This thesis describes work that consists of the following scientific contributions: * Martin was wrong * New lines * Weakest transition * Test of QED * Partial resolution of QD which didn't answer much and isn't decisive re: theory * work towards a new regime of condensed matter simulation

- future specroscopy - prospects for helium 3
- Lattices - possible directions
- Quantum correlations & foundations experiments

A personal reflection. Was lured in to the academy by the promise of questions like 'what is the difference between simplicity and complexity' - when are things simple? When is something intrinsically hard to represent, even if it exists effortlessly in its own right? This drew me to lattice - to build something with the hands that would be so elusive for theory and computing. But yeah - that might have been possible, but I hadn't the background to make reasonable progress in the three year timeframe of an Australian PhD. Also, frankly, I didn't have the tuition or support and so was left alone for most of the time, crushing motivation and without praise and squirreled my time away in a simulation that was much more to my theoretical tastes. But hey. I have to find a nice way to dress this up. Most of these words won't make it. So having got these ones out of the way, the hope is that I can move on from them and think more deliberately about what it is that I would say here.

The chronological order of work is reversed. I should perhaps detail the actual sequence of events - and frame them as pragmatic decisions from which I learned some useful things about scoping projects properly. There isn't really much that window dressing can add here. But that's okay - rather than telling the entire truth, just tell enough of it. But don't let the complexity frighten you out of doing your best to be honest, at least in this tiny sliver, the final vestiage of the self-expression that you'd hoped you'd find the opportunity to explore. This has been an exercise in shedding the ego, however incomplete that process may yet remain.

###A critical reading of science Technology evidently brings us great things. But let us not lose sight of the implicit 'right to know' - that we still embody the notion of a conquest over nature, of mastery of the other, the greater, the ultimately incomprehensible. Let us not fall victim to our own arrogances, and recall that in our turbulent times, our investigations come at cost. The nature of reality will, according

to our ultimate foundations, remain. But the conditions of society in which we have the ability to pursue them are not guaranteed. One can never predict the outcomes of discoveries, or what miraculous things may be born of new technologies, but in the problem of allocating compute power from human wetware - which still retains a certain je ne sais quois that has not been replicated by industrial-scale algorithms running in silico - we should be mindful of the hubris of endless pursuit of the mastery of nature. This remains ingrained in our mythology - that more advanced technology is always worth the price that is paid. In the limit of free, clean energy and post-scarcity manufacture whereby human labour is eliminated, this may be true. But, unlike the atoms in this thesis, we do not live in vacuum.

"We shall not cease from exploration
And the end of all our exploring
Will be to arrive where we started
And know the place for the first time."
- T. S. Eliot